

**Advanced Automated HVAC Fault
Detection and Diagnostics
Commercialization Program**

**Final Field Emulation Report and Final
Algorithm Test Report**

CONSULTANT REPORT

Prepared For:
California Energy Commission
Public Interest Energy Research Program

Prepared By:
Field Diagnostic Services, Inc.



Arnold Schwarzenegger, *Governor*

December 2006
Contract #500-03-030
Subtask 5.5b & 5.5e
Deliverable

CALIFORNIA ENERGY COMMISSION

Prepared By:

Purdue University – Sponsored Program Services
James Braun, Ph.D.
Adam Wichman
302 Wood Street
West Lafayette, IN 47907

Program Director

Vernon Smith
Architectural Energy Corporation
Boulder, Colorado
Commission Contract No. 500-03-030

Prepared For:

Chris Scruton

Contract Manager

Ann Peterson

PIER Buildings Program Manager

Nancy Jenkins

Office Manager

ENERGY EFFICIENCY RESEARCH OFFICE

Martha Krebs, Ph.D.

Deputy Director

**ENERGY RESEARCH AND DEVELOPMENT
DIVISION**

B. B. Blevins

Executive Director

DISCLAIMER

This report was prepared as the result of work sponsored by the California Energy Commission. It does not necessarily represent the views of the Energy Commission, its employees or the State of California. The Energy Commission, the State of California, its employees, contractors and subcontractors make no warrant, express or implied, and assume no legal liability for the information in this report; nor does any party represent that the uses of this information will not infringe upon privately owned rights. This report has not been approved or disapproved by the California Energy Commission nor has the California Energy Commission passed upon the accuracy or adequacy of the information in this report.

TABLE OF CONTENTS

INTRODUCTION	4
<u>BACKGROUND</u>	4
<u>GOALS</u>	5
EXPERIMENTAL SETUP	5
<u>UNIT INFORMATION</u>	5
<u>INSTRUMENTATION AND DATA ACQUISITION</u>	6
<u>DAMPER OPERATION AND CONTROL</u>	8
EXPERIMENTAL PROCEDURES AND RESULTS	10
<u>TEST PROCEDURE</u>	10
<u>TEST MATRIX</u>	10
<u>DATA EVALUATION</u>	15
<u>IMPACT OF NUMBER AND LOCATION OF SENSORS ON MEASURED MIXED AIR STATE</u>	16
FDD ALGORITHM EVALUATION METHOD	21
<u>ECONOMIZER MODEL</u>	21
<u>FDD ALGORITHM EVALUATION PROCESS</u>	26
FDD ALGORITHM AND EVALUATION RESULTS	28
<u>ALGORITHM DESCRIPTION</u>	28
<u>EVALUATION RESULTS FOR THE FDSI ALGORITHM</u>	29
<u>SUGGESTED FDD ALGORITHM IMPROVEMENTS</u>	37
<u>EVALUATION OF THE IMPROVED ALGORITHM</u>	40
<u>A DESCRIPTION OF OTHER POSSIBLE ECONOMIZER FDD METHODS</u>	47
SUMMARY, CONCLUSIONS, AND RECOMMENDATIONS	48
<u>SUMMARY AND CONCLUSIONS</u>	48
<u>RECOMMENDATIONS</u>	49
NOMENCLATURE	50
REFERENCES	51

INTRODUCTION

Background

Economizers are incorporated into building HVAC systems to decrease energy consumption during mild weather periods by using outdoor air to meet the cooling load in lieu of the mechanical cooling system. In fact, many commercial buildings require some cooling year round due to heat produced from office equipment, lighting, and computers (Katipamula et al. 1999). In certain climates, buildings can derive a large amount of cooling from an economizer system. In addition to energy savings, economizers can improve indoor air quality (IAQ) for the building occupants during the portion of the year when they are operational. In one case study, Fisk et al. (2005) predicted 6.3% energy savings for an economizer in a medium sized, two-story office building and 19.1% labor cost savings due to improved worker productivity and reduced sick leave.

According to Katipamula et al. (1999), an economizer system is comprised of four parts: a damper system, an economizer controller, a temperature controller, and a minimum position limiter. These elements are depicted in Figure 1. The dampers are used to allow outside, fresh air into the building while exhausting indoor air. The economizer controller determines when to allow outdoor air into the building for cooling, and the temperature controller's purpose is to limit the amount of outdoor air coming into the building when outdoor conditions would result in a low supply air temperature (SAT). Last, the minimum position limiter insures that the damper system allows enough outdoor air into the building to ensure favorable IAQ. This minimum amount of outdoor air is also referred to as the minimum outdoor air fraction (minOAF).

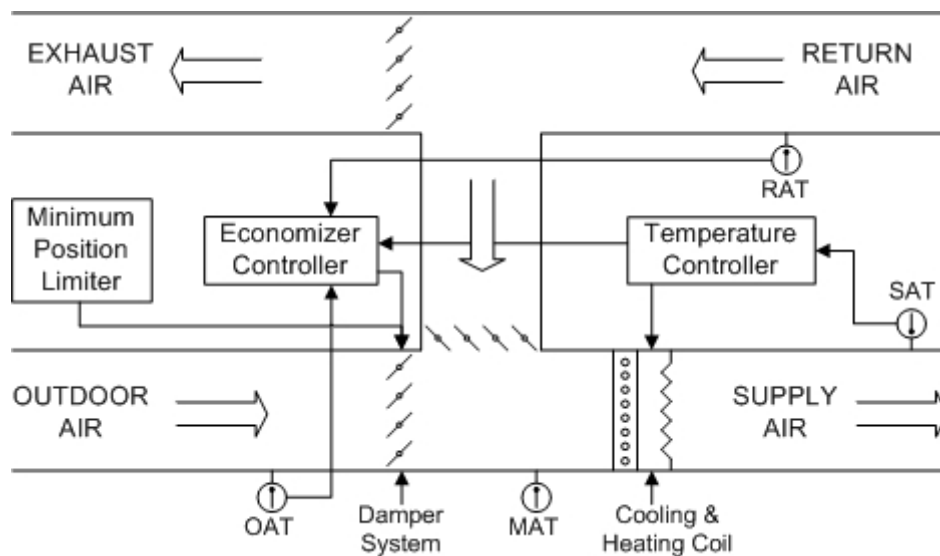


Figure 1: Economizer schematic.

There are two common control strategies for economizer systems: changeover or high-limit control, and differential control (Friedman, 2001). With changeover control, the ambient dry or wet bulb temperature is compared with an outdoor air setpoint to determine if the economizer should be in “economizer mode.” The outdoor state must be sufficiently “cooler” than the expected return air state to ensure that ventilation air will

reduce the equipment cooling load. With differential control, the outdoor state (dry or wet bulb temperature) is compared with a measurement of the return air state (dry bulb or wet bulb temperature) to determine if the economizer should be enabled. In economizer mode, the dampers are actively adjusted using a feedback controller to achieve a specified mixed air temperature (MAT) referred to as the mixed air setpoint (MAsetpt). When the economizer is not enabled during occupancy, then the dampers revert to a minimum position to allow a minimum amount of outdoor air.

Economizer faults can develop through normal operation or be present due to installation errors. Faults can increase energy costs and/or reduce indoor air quality. For example, a stuck damper that is fully open on a hot summer day leads to increased cooling requirements and costs. On the other hand, a stuck damper that is fully closed can degrade IAQ leading to decreased worker productivity and higher business costs. Cowan (2004) published a study of commercial rooftop air conditioners in the Pacific Northwest where half of the inspected economizers had faults. Problems with the economizers included damper faults, controller faults, and sensor faults. Automated fault detection and diagnostic (FDD) techniques has the potential identify economizer faults using low cost measurements leading to reduced energy consumption and improved IAQ.

Goals

This study had two major goals. The first goal was to identify the appropriate number of and location for sensors to properly characterize the mixed air state for use with refrigeration cycle diagnostic algorithms. Non-uniformities in the mixed air state depend on damper positions and outdoor air conditions and can have a large impact on diagnostic performance. The second goal was to perform an extensive evaluation of an existing economizer FDD algorithm that was developed by Field Diagnostic Services, Inc. (FDSI) and to recommend improvements. In order accomplish these goals, extensive testing was performed on air side of a rooftop air conditioning unit equipped with an economizer.

EXPERIMENTAL SETUP

Unit Information

The experiments were performed on a Trane 5-ton rooftop unit (model number TSC060A) equipped with an economizer (model number BAYECON085A). The economizer used in this setup was designed to be packaged and controlled in combination with the mechanical cooling system, which is termed an integrated system (Katipamula et al. 1999). The rooftop unit was setup inside a psychrometric chamber at the Herrick Laboratories, Purdue University, to simulate outdoor conditions. A diagram of the experimental setup is shown in Figure 2. The unit was elevated off the floor so that return air ducts could be attached under the unit and then connected to another psychrometric chamber that simulated indoor conditions. A duct was attached to the outdoor air inlet to the economizer for measurement purposes. The indoor supply duct from the rooftop unit was connected to an air flow measurement system that contained calibrated flow nozzles. In addition to the installed rooftop indoor fan, an external

variable fan was utilized to overcome pressure drop in the air measurement system achieve the range of required flow rates.

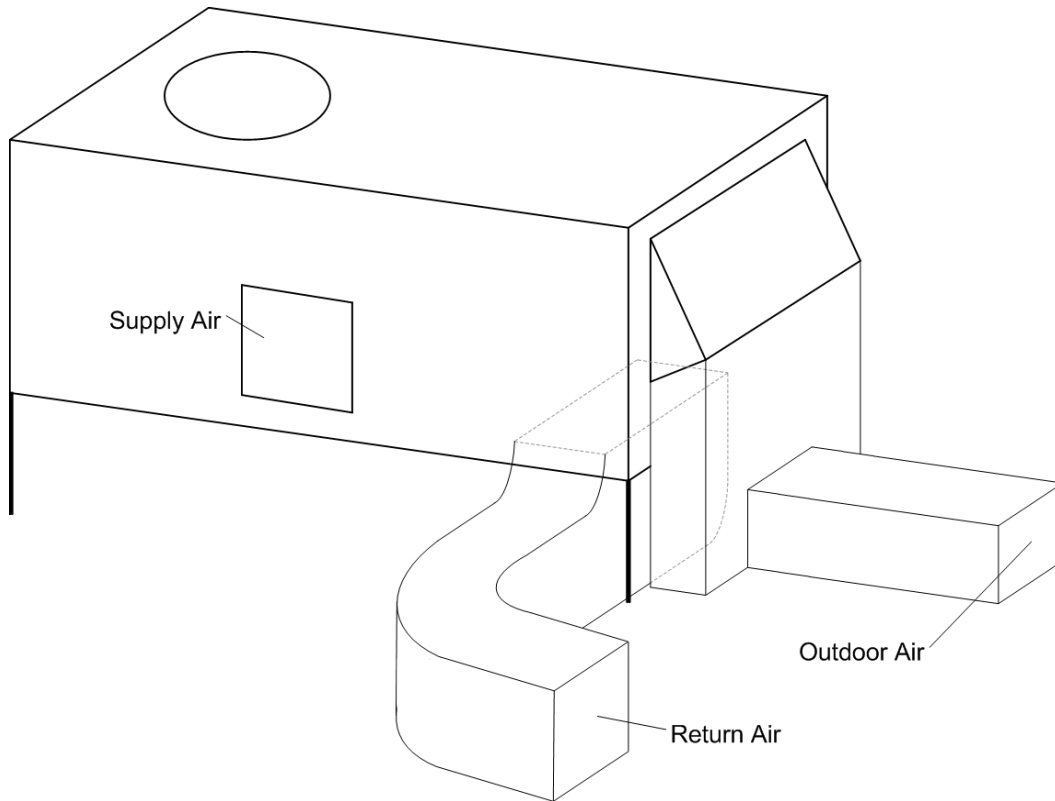


Figure 2: Economizer experiment ducts setup (not to scale).

Instrumentation and Data Acquisition

Four different measurement grids were set up in the unit with a total of 33 T-type thermocouples each having a rated accuracy of $\pm 1.8^{\circ}\text{R}$ ($\pm 1\text{ K}$). Nine thermocouples were arranged on grids at both the outdoor and return air inlets. Inside the packaged air conditioner, there is a small chamber whose purpose is to mix the outdoor and return air streams before crossing the evaporator coil. Since mixed air measurements need to be made before the air crosses the coil, all of the mixed air instrumentation was placed on a grid directly in front of the coil. Fifteen thermocouples were placed in five rows and three columns symmetrically across the evaporator coil to measure the mixed air temperature. Air sampling tubes used to measure dew point were attached to the center of both the outdoor and return air measurement grid. Ten sampling tubes were also fastened to the grid with two tubes in each of the five rows that contained the temperature sensors. The sampling tubes were connected to a General Eastern dew point hygrometer (model number D-2) via an air sampling pump (model number SSM-1). Figure 3 below shows the mixed air measurement grid, and Figure 4 provides a picture of the fully assembled measurement grid.

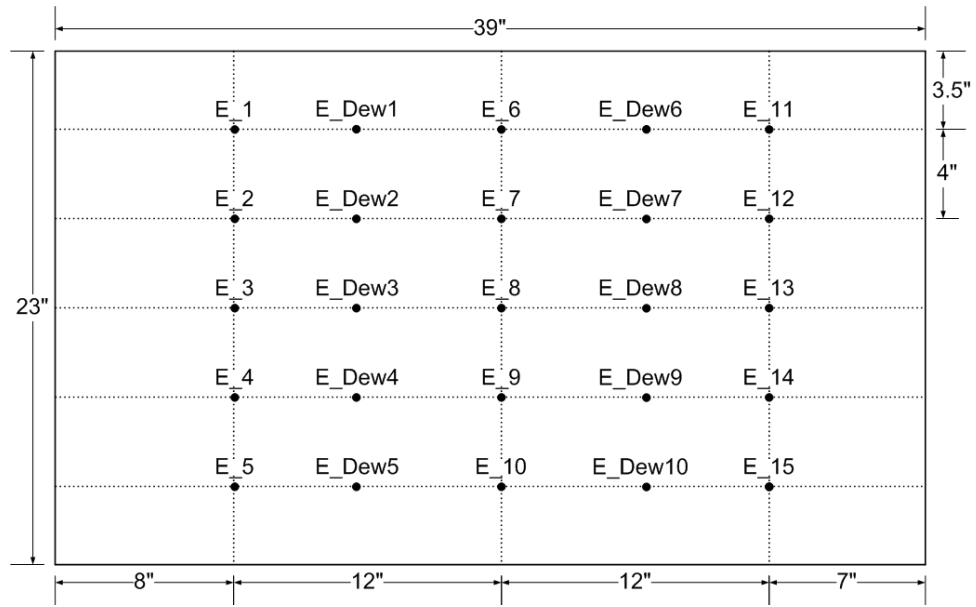


Figure 3: Evaporator air measurement grid.



Figure 4: Photo of the mixed air measurement grid.

To correctly determine the outdoor air fraction (OAF), two air mass flow rate measurements were required. The supply air from the rooftop unit was routed to a bank of three ASME standard nozzles for measurement. A thermal dispersion measurement

system manufactured by Ebtron (model number GTx116-PC) was used to determine outdoor air flow rates. This device has a rated accuracy of $\pm 0.1\%$ of measurement, yielding extremely accurate air flow measurements even at low air velocities. The supply, and outdoor air mass flow rates were used to calculate the return air flow rate and OAF assuming no significant leakage in the duct work. To minimize leakage, each joint and seam in the ducts was securely taped.

Since the air flow setup for the system is inherently imbalanced, pressurization of the indoor room was inevitable. A Dwyer series 603A differential pressure transducer was used to measure the pressure imbalance between the two psychrometric chambers.

For data acquisition, a Hewlett Packard HP75000 Series B was used for collecting the instrument data. The software, HPVVEE, was utilized to read, display, and record the experimental data. Data was sampled and recorded at five second intervals.

Damper Operation and Control

To collect a data set that incorporates all modes of economizer operation, both unfaulted and faulted, the economizer logic module was removed from the damper motor and economizer damper was configured so it could be manually controlled. The economizer motor required a 24 volt AC source to power the motor. The damper position was controlled by supplying a 2-10 volt, variable DC voltage source to the motor. The motor had a DC voltage output indicating damper position using the same 2-10 volt scale as the input, where a 2V input returns the damper minimum position of about 5% outdoor air and the 10V input returns a damper position of about 75% outdoor air. Due to the high air flow rates tested and the flimsy construction of the return air damper, significant leakage passed the return damper when it was closed at the 10V motor input preventing the economizer system from achieving higher OAFs than 75%. With this setup, the control voltage could be varied to position the damper wherever it was required. Figures 5 and 6 are pictures of the damper at the minimum position and an almost fully open position.



Figure 5: Photo of the economizer damper at the minimum position.



Figure 6: Photo of the economizer damper at an almost fully open position.

EXPERIMENTAL PROCEDURES AND RESULTS

Test Procedure

It was not necessary to run the mechanical cooling system in the rooftop unit since the goals only included issues related to the uniformity of air inlet conditions to the coil and economizer operation. The doors on the psychrometric chambers had to be left slightly open to keep the pressure difference between the rooms at a minimum. It was found that by closing the chamber doors, outdoor air flow would drop significantly making it impossible to test the high OAF conditions indicated on the test matrix. Leaving the doors slightly open did not have a significant effect on the chamber's ability to control air temperature and humidity. To set up a test, the indoor and outdoor psychrometric chambers were utilized to control the temperature and relative humidity (RH) for the outdoor and return air streams. With the chambers active and at steady state conditions and the fans set to the required air flow rate, the economizer damper position could be varied over its entire range. For each condition and damper position, temperature data was collected continuously. However, only one dew point hygrometer was available so taking dew point data at all 13 points, which includes the outdoor air, return air, supply air, and ten mixed air points, in the test setup required manually connecting the sampling tubes one at a time to the hygrometer. Data was collected for several minutes with each dew point sampling tube connected for each damper position. Collection of data at a test point was completed after all of the dew point data was collected for a given set of air conditions and damper position.

Test Matrix

The testing matrix was initially designed to collect a wide spectrum of data to be used in evaluating the economizer FDD algorithm. The ASHRAE Fundamentals Handbook was consulted to determine appropriate ranges of outdoor RH to test depending on the OAT (ASHRAE 2001). Figure 7 shows a plot of maximum summer temperatures and average temperatures versus a corresponding average humidity that was generated from data for several cities across the United States. This plot shows approximate upper and lower bounds of RH based on an outdoor air temperature and was a basis for selecting a range of relative humidities to test at different OATs.

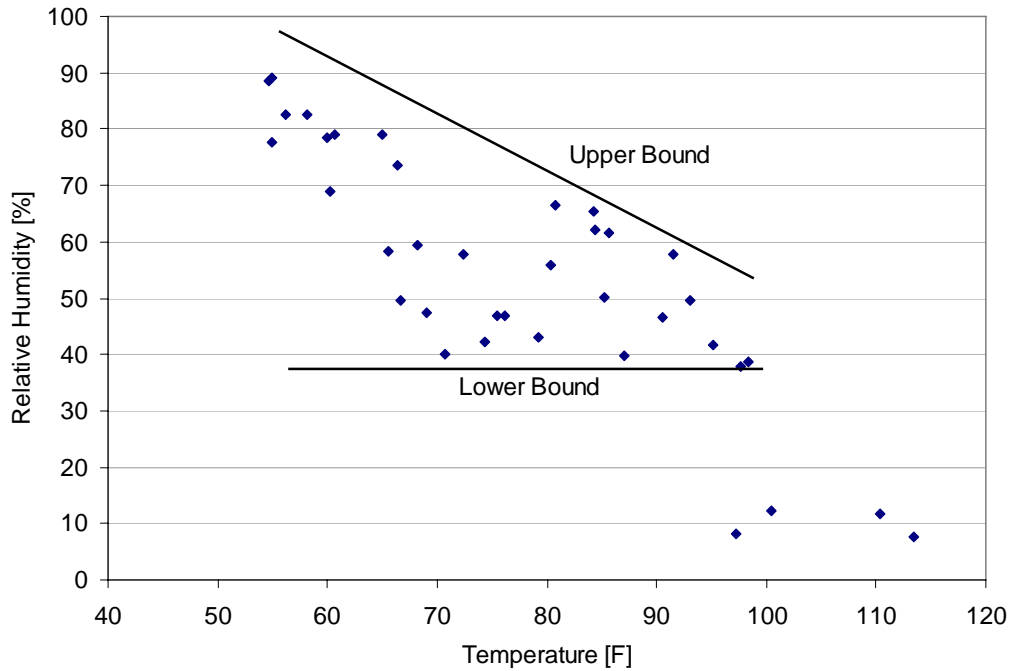


Figure 7: Average and maximum temperatures for several cities versus their respective average relative humidity.

Table 1 shows the original test matrix that was developed to consider a wide range of combinations of room conditions and damper positions. The economizer was tested for both heating and cooling modes of operation which means that two different ranges of outdoor air temperatures were tested. Many relative humidities in the matrix were considered “dry,” which means that the humidity level was maintained below 40%. The total air flow of the system was to be varied over a range of 1200 to 2000 CFM (0.566 to 0.944 m³/s), and the damper position was to be varied from 5-75 percent outdoor air (%OA) in 8 increments. Indoor conditions were held constant depending on the mode being tested.

Table 1: Original economizer test matrix.

Mode	Total Air Flow (CFM)	%OA	OAT	Outdoor RH (%)	RAT	Indoor RH (%)
			(F, C)		(F, C)	
Cooling	1200	5-75%	55 (12.8)	40-100%	75 (23.9)	50
Cooling	1200	5-75%	65 (18.3)	40-100%	75 (23.9)	50
Cooling	1200	5-75%	75 (23.9)	40-100%	75 (23.9)	50
Cooling	1200	5-75%	85 (29.4)	40-100%	75 (23.9)	50
Cooling	1200	5-75%	95 (35)	40-60%	75 (23.9)	50
Cooling	1200	5-75%	105 (40.6)	dry	75 (23.9)	50
Cooling	1200	5-75%	115 (46.1)	dry	75 (23.9)	50
Heating	1200	5-75%	20 (-6.7)	dry	70 (21.1)	dry
Heating	1200	5-75%	30 (-1.1)	dry	70 (21.1)	dry
Heating	1200	5-75%	40 (4.4)	dry	70 (21.1)	dry

Cooling	1600	5-75%	55 (12.8)	40-100%	75 (23.9)	50
Cooling	1600	5-75%	65 (18.3)	40-100%	75 (23.9)	50
Cooling	1600	5-75%	75 (23.9)	40-100%	75 (23.9)	50
Cooling	1600	5-75%	85 (29.4)	40-100%	75 (23.9)	50
Cooling	1600	5-75%	95 (35)	40-60%	75 (23.9)	50
Cooling	1600	5-75%	105 (40.6)	dry	75 (23.9)	50
Cooling	1600	5-75%	115 (46.1)	dry	75 (23.9)	50
Heating	1600	5-75%	20 (-6.7)	dry	70 (21.1)	dry
Heating	1600	5-75%	30 (-1.1)	dry	70 (21.1)	dry
Heating	1600	5-75%	40 (4.4)	dry	70 (21.1)	dry
Cooling	2000	5-75%	55 (12.8)	40-100%	75 (23.9)	50
Cooling	2000	5-75%	65 (18.3)	40-100%	75 (23.9)	50
Cooling	2000	5-75%	75 (23.9)	40-100%	75 (23.9)	50
Cooling	2000	5-75%	85 (29.4)	40-100%	75 (23.9)	50
Cooling	2000	5-75%	95 (35)	40-60%	75 (23.9)	50
Cooling	2000	5-75%	105 (40.6)	dry	75 (23.9)	50
Cooling	2000	5-75%	115 (46.1)	dry	75 (23.9)	50
Heating	2000	5-75%	20 (-6.7)	dry	70 (21.1)	dry
Heating	2000	5-75%	30 (-1.1)	dry	70 (21.1)	dry
Heating	2000	5-75%	40 (4.4)	dry	70 (21.1)	dry

In order to reduce the time required to perform the experiments, the original test matrix was modified to eliminate test conditions that were deemed unnecessary. The first set of tests conducted were the tests in heating mode. The heating mode tests were conducted at 20°F, 30°F, and 40°F OAT and 70°F RAT. After the tests were complete, mixed air temperature data, comprised of an average of all 15 mixed air sensors, was plotted as a function of outdoor air fraction for a specified OAT. Data from the total air system flow rates was compared as shown below for the 30°F OAT case in Figure 8. At all three outdoor air temperatures, as the total system air flow rate changes, the mixed air temperature remains about the same for a specified OAF. This trend held true for the other two heating mode OATs, and because of this, it was decided that it was not necessary to conduct the cooling mode tests at all three total system air flow rates. Instead, only the 2000 CFM flow rate was used for tests in cooling mode.

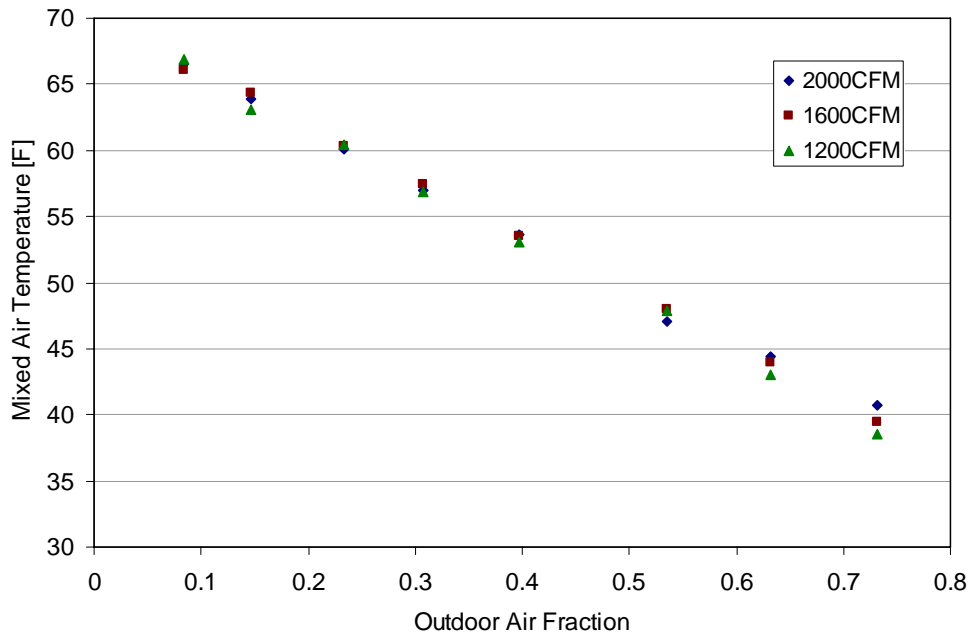


Figure 8: Average mixed air temperature as a function of outdoor air fraction for three different total system air flow rates at 30°F outdoor air temperature.

A very time consuming aspect of the tests was determination of the dew points. Initially, it was thought that all 13 sampling tubes would be used at every test point to get dew point measurements of the outdoor air, return air, supply air, and at 10 locations across the evaporator to represent the mixed air. In order to speed up the experiments, the accuracy of measuring dew point at two positions across the evaporator was evaluated and found to be sufficient. Using this updated method, only five sampling tubes needed to be measured at any given room conditions and damper position. The results of this validation are presented in the section labeled “Impact of Number and Location of Sensors on Measured Mixed Air State.”

It was also found that it was unnecessary to perform tests at eight different damper positions at every combination of room conditions. Results presented in both Figure 9 demonstrates that average MAT varies nearly linearly with OAF. In addition, OAF varies linearly with the damper position. With this linear behavior, four damper positions were enough to cover the whole range of damper positions and clearly show trends.

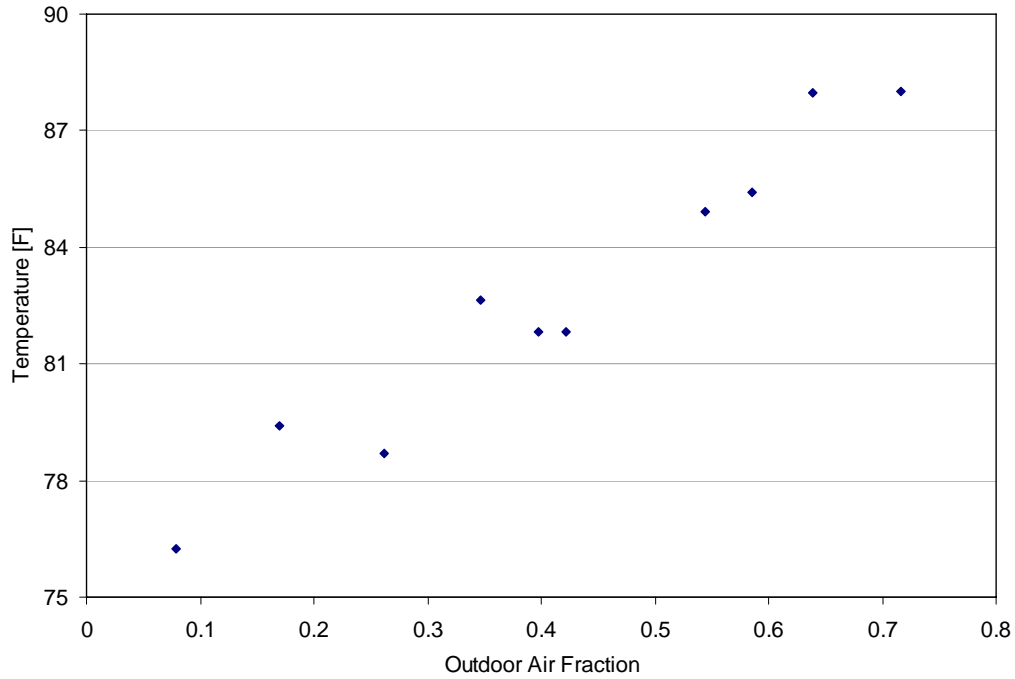


Figure 9: Average mixed air temperature as a function of outdoor air fraction at 95°F outdoor air temperature.

With these simplifications, the test matrix was revised to reflect the removal of unneeded test points resulting in a greatly reduced testing time. Table 2 shows the revised test matrix that represents all the data points that were collected.

Table 2: Revised Economizer Test Matrix.

<u>Mode</u>	<u>Total Air Flow (CFM)</u>	<u>%OA</u>	<u>OAT</u> <u>(F, C)</u>	<u>Outdoor RH (%)</u>	<u>RAT</u> <u>(F, C)</u>	<u>Indoor RH (%)</u>
Cooling	2000	5-75%	55 (12.8)	40-75%	75 (23.9)	50
Cooling	2000	5-75%	65 (18.3)	40-100%	75 (23.9)	50
Cooling	2000	5-75%	75 (23.9)	40-100%	75 (23.9)	50
Cooling	2000	5-75%	85 (29.4)	20-75%	75 (23.9)	50
Cooling	2000	5-75%	95 (35)	20-40%	75 (23.9)	50
Cooling	2000	5-75%	105 (40.6)	dry	75 (23.9)	50
Cooling	2000	5-75%	115 (46.1)	dry	75 (23.9)	50
Heating	2000	5-75%	20 (-6.7)	dry	70 (21.1)	dry
Heating	2000	5-75%	30 (-1.1)	dry	70 (21.1)	dry
Heating	2000	5-75%	40 (4.4)	dry	70 (21.1)	dry
Heating	1600	5-75%	20 (-6.7)	dry	70 (21.1)	dry
Heating	1600	5-75%	30 (-1.1)	dry	70 (21.1)	dry
Heating	1600	5-75%	40 (4.4)	dry	70 (21.1)	dry
Heating	1200	5-75%	20 (-6.7)	dry	70 (21.1)	dry
Heating	1200	5-75%	30 (-1.1)	dry	70 (21.1)	dry
Heating	1200	5-75%	40 (4.4)	dry	70 (21.1)	dry

Data Evaluation

One approach that was used to check the validity of the data was to compare OAF values determined directly from air flow measurements to OAF data calculated from temperature data. It can be shown using energy and mass balances on the mixing chamber within the economizer that the OAF can be determined from temperature measurements using the following relation (Friedman and Piette, 2001).

$$OAF = \frac{MAT - RAT}{OAT - RAT}$$

OAF determined in this manner is often utilized as a low-cost measure of ventilation flow.

Figure 10 shows calculated OAF as a function of the measured OAF for data obtained in this project. For these results, all of the available thermocouple measurements were used to determine average temperatures. Overall, the calculated OAF was within 8% of measured OAF over the range of conditions considered. On average, the calculated OAF deviated from the measured values by 2%.

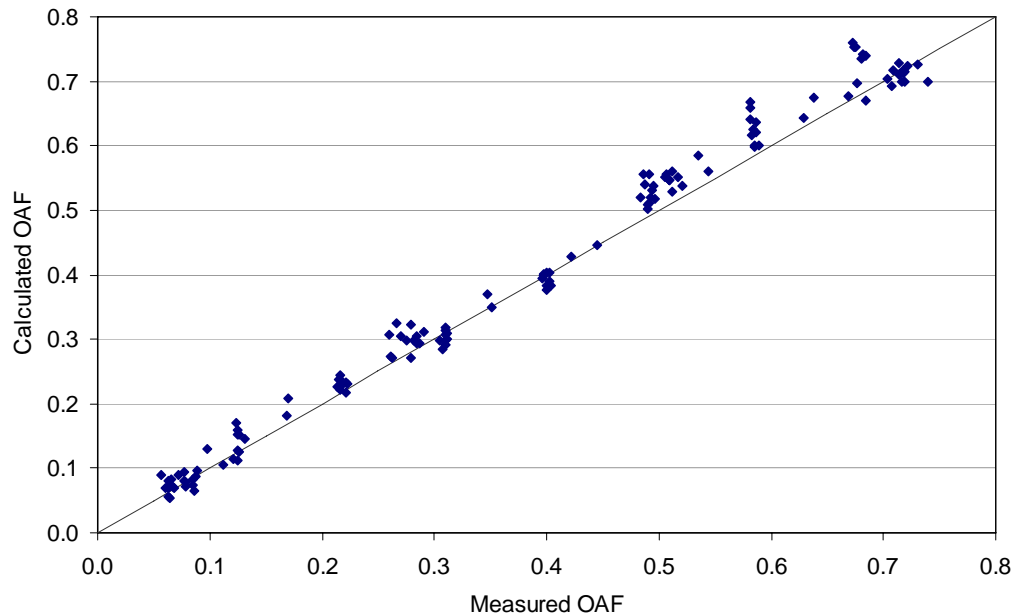


Figure 10: Calculated OAF as a function of measured OAF.

An overall energy balance on the economizer was also used to compare calculated mixed air enthalpies with values determined from average mixed air dry bulb and dew point temperature measurements. The calculated mixed air enthalpy (Mh) was obtained using

$$Mh = \frac{\dot{m}_{OA}}{\dot{m}_{Total}} Oh + \frac{\dot{m}_{RA}}{\dot{m}_{Total}} Rh$$

where Oh is the outdoor air enthalpy, Rh is the return air enthalpy, \dot{m}_{OA} is the mass flow rate of the outdoor air, and \dot{m}_{RA} is the mass flow rate of the return air.

Figure 11 compares average mixed air enthalpies determined from an energy balance and measurements. All 15 dry bulb and 10 dewpoint mixed air measurements were used in determining Mh. Overall, the calculated and measured Mh values differ by at most 8.7% and on average differ by 1.8%.

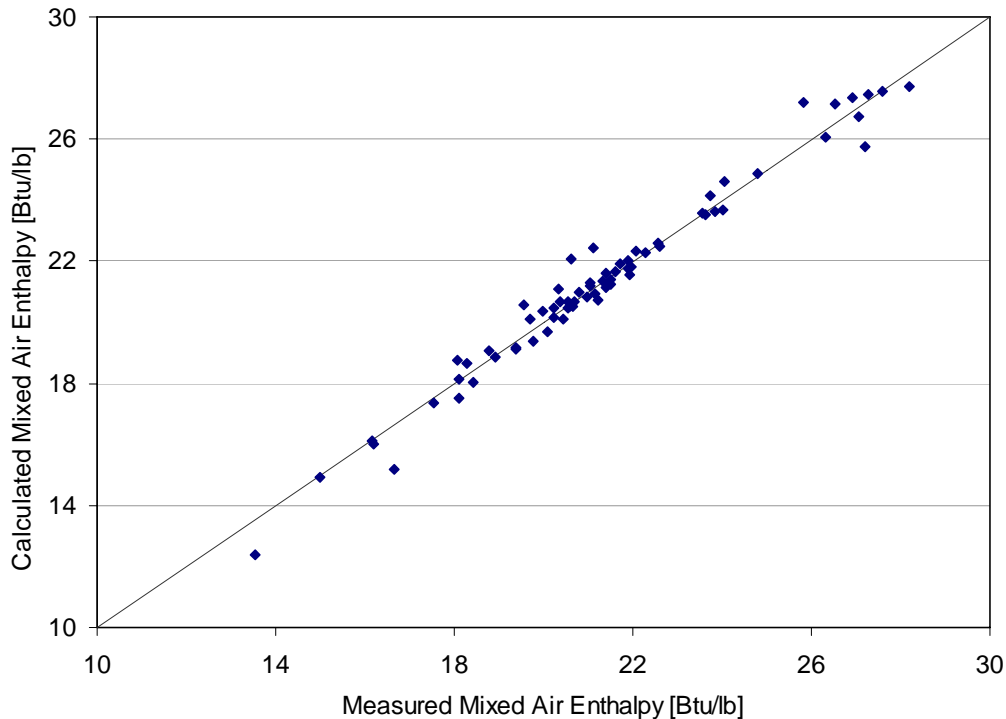


Figure 11: Measured Mh versus calculated Mh.

Impact of Number and Location of Sensors on Measured Mixed Air State

In addition to collecting data for the purpose of evaluating an economizer FDD algorithm, one of the major goals of the experiments was to evaluate the accuracy of using just a few temperature and dew point sensors to represent the mixed air condition. For the experiments, 15 thermocouples were positioned across the evaporator as well as 10 sampling tubes for the purposes of collecting dew point measurements (see Figure 3). Using all of the data collected from every mixed air measurement, it is possible to determine the best combinations of a limited number of sensors to represent the mixed air condition.

The first step in this process involved the evaluation of using two dew point measurements as compared with the ten depicted in Figure 3. The evaluation was done for cooling mode tests with the outdoor air at 95°F (35°C) and 40% RH and the indoor air at 75°F (23.9°C) and 50% RH for ten different damper positions ranging from 5-75 %OA. It was important to consider different damper positions because of the impact on the mixing process. Through analysis of the data, it was found that the use of two dewpoint measurements located at the horizontal centerline of the mixing chamber

(E_Dew3 and E_Dew8 in Figure 2) provided the best estimate of average dewpoint measurement. Figure 12 shows the difference between the full 10-point and 2-point centerline dew point measurements as a function of OAF. The maximum difference was less than 2.5°F with an average difference less than 0.7°F. In fact, the two horizontal centerline measurements were nearly the same in all cases and it is recommended that a single centerline humidity measurement be used for the mixed air condition. For the remainder of this report, the two horizontal centerline dewpoint measurements were used to determine mixed air enthalpies.

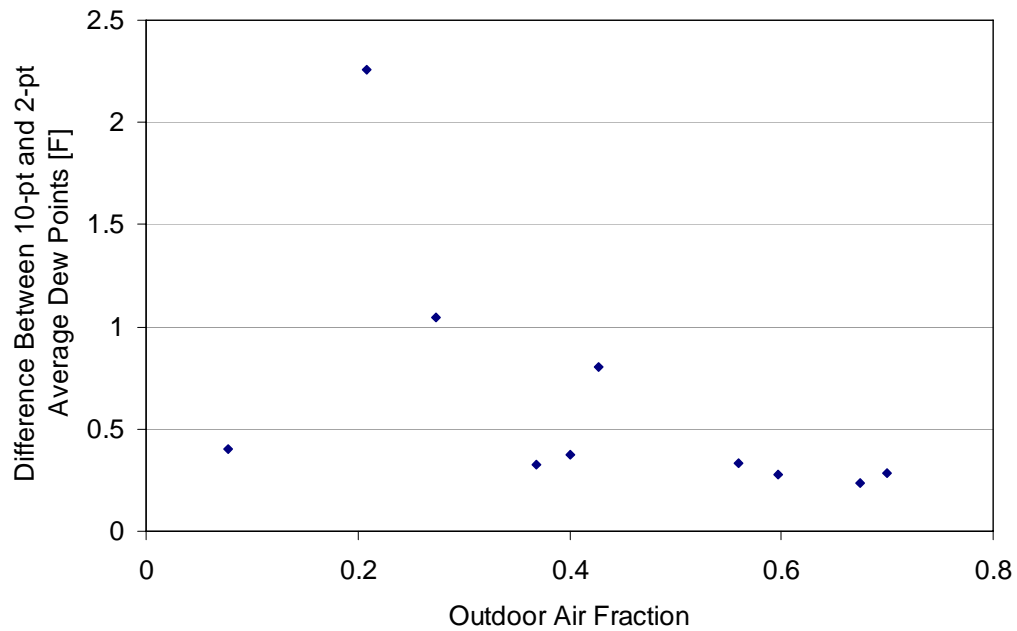


Figure 12: Percent error in using a two-point dew point measurement as a function of outdoor air fraction.

Figure 13 shows differences between mixed air enthalpy determined from an energy balance on the economizer and values determined from averages of the 15 mixed air dry bulb and 2 dew point temperature measurements. The maximum difference is less than 1.1 Btu/lb (2.56 kJ/kg) and typically less than 0.4 Btu/lb. This is further evidence that a single-point or two-point mixed air dew point measurement is reasonable.

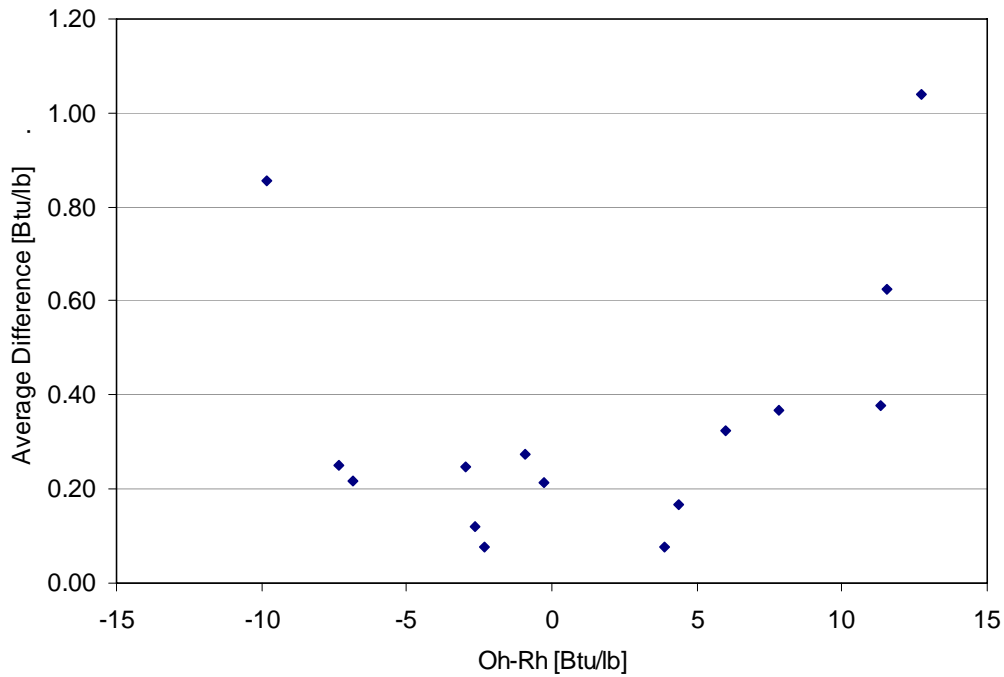


Figure 13: Average difference between Mh determined with 2 dewpoint temperatures and Mh calculated from an energy balance as a function of the difference between Oh and Rh.

In order to evaluate the best location and number for mixed air dry bulb temperatures, a variety of different cases were considered. It was found that there are very large errors associated with using a single-point measurement, even when located in the duct centerline. In fact, it is necessary to utilize four temperature measurements in order to obtain accurate average mixed air temperatures. Several combinations of four temperature sensors were analyzed and compared with 15-point and single-point measurement schemes. Table 3 gives a simplified measurement grid showing numbered positions of temperature sensors and Table 4 shows the combinations of sensor locations that were examined.

Table 3: Mixed air temperature measurement grid.

1	6	11
2	7	12
3	8	13
4	9	14
5	10	15

Table 4: Sensor combinations evaluated.

<u>Measurement Method</u>	<u>Sensor Locations</u>
1	3,7,9,13
2	3,6,7,13
3	2,4,12,14
4	8

To evaluate the different temperature measurement methods, the absolute value of the differences between averages for the sensor combination of a particular method and averages for all 15 sensors were determined as

$$\Delta T = \left| \frac{\sum_i T_i}{n} - \frac{\sum_{j=1}^{15} T_j}{15} \right|$$

where i represents each sensor location used in the measurement method and n is the number of sensors used in the method.

The ΔT s were calculated for each experimental data point and average values were determined for common outdoor and indoor air conditions. Average ΔT s are plotted as a function the difference between OAT and RAT in Figure 14. As would be expected, the average differences between each measurement method and the 15-point measurement decrease nearly to zero as the difference between the OAT and RAT approaches zero. When the OAT and RAT are significantly different, then the best 4-point method uses the most widely and evenly spaced sensor combination of 3, 6, 10, and 13. However, the other three 4-point methods also gave good results. The use of a single sensor along the centerline of the duct does not work well give a maximum error of about 5°F (2.78°C). Using a single sensor in other locations gave even worse results.

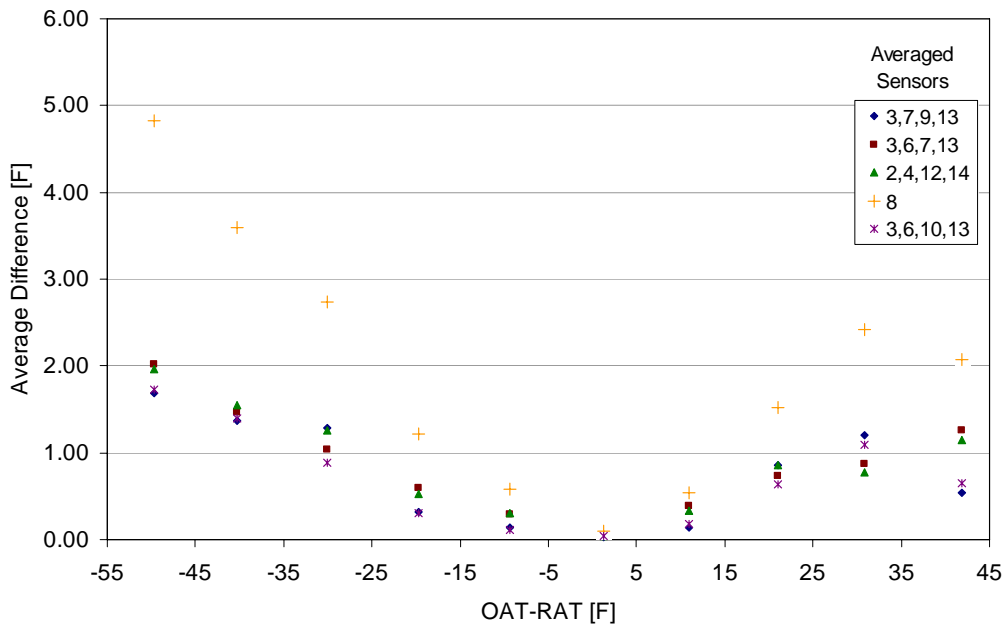


Figure 14: Averaged temperature differences between the 15-point average and averages for reduced numbers of sensors as a function of OAT-RAT.

Figures 15 and 16 below show results for the most accurate and least accurate measurement methods with standard deviation bars. The standard deviations characterize the variations in the ΔT s at each set of outdoor and return air conditions due to variations in damper position. In particular, there can be extremely large errors associated with using a single-point measurement for the mixed air temperature. Overall, a single point measurement of temperature is only accurate at small differences between OAT and RAT. A 4-point configuration for mixed air temperature sensors is recommended.

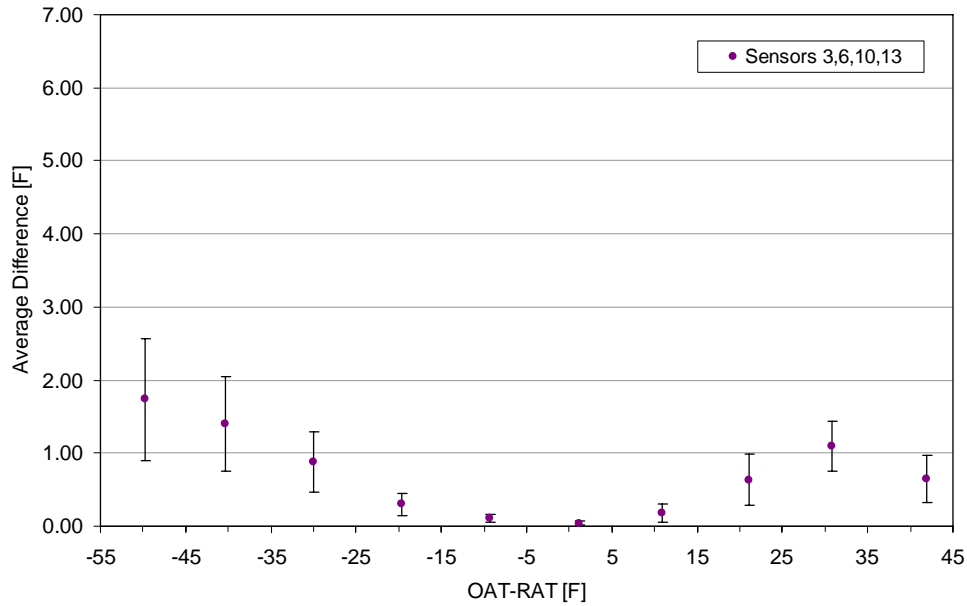


Figure 15: Average difference plot for the sensor combination of 3, 6, 10, and 13 with standard deviation bars.

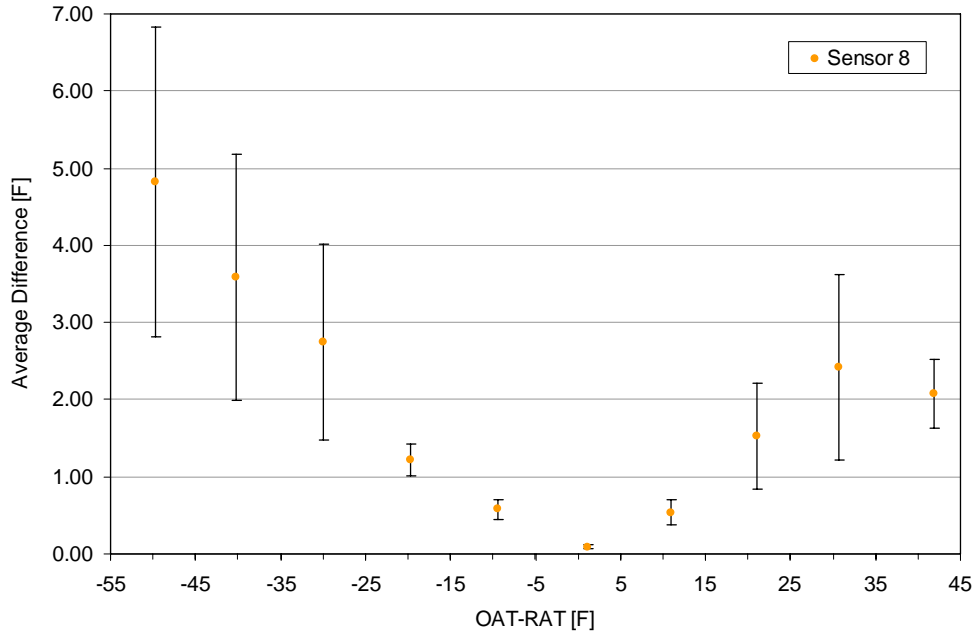


Figure 16: Average difference plot for the sensor 8 with standard deviation bars.

FDD ALGORITHM EVALUATION METHOD

In order to evaluate FDD algorithms, the experimental data was used to create a computer model of the economizer system that allows simulations of common faults. This section describes the economizer model, the fault matrix, and the process used to evaluate the FDD algorithm.

Economizer Model

The economizer model contains three parts: 1) a mapping between mixed air temperature and damper position, outdoor conditions, and return conditions, 2) an economizer controller model, and 3) a fault implementer.

Models were developed in order to predict the “sensed” mixed air temperature for different choices for number and location of sensors in terms of outdoor air fraction and temperature and return air temperature. For each combination of sensors considered, the following second-order linear regression model was employed to predict the average mixed air temperature.

$$\begin{aligned}
 MAT = & a_1 + a_2 OAT + a_3 (OAT)^2 + a_4 RAT + a_5 (RAT)^2 + a_6 OAF + a_7 (OAF)^2 \\
 & + a_8 (OAT)(RAT) + a_9 (OAT)(OAF) + a_{10} (RAT)(OAF)
 \end{aligned}$$

where a_{1-10} are the coefficients generated by the regression. Since separate models are employed for different choices of mixed air sensors, the regression model captures the effect of imperfect mixing inside the mixing chamber. The process of generating the regression equation for a given choice of sensors is summarized in Figure 17.

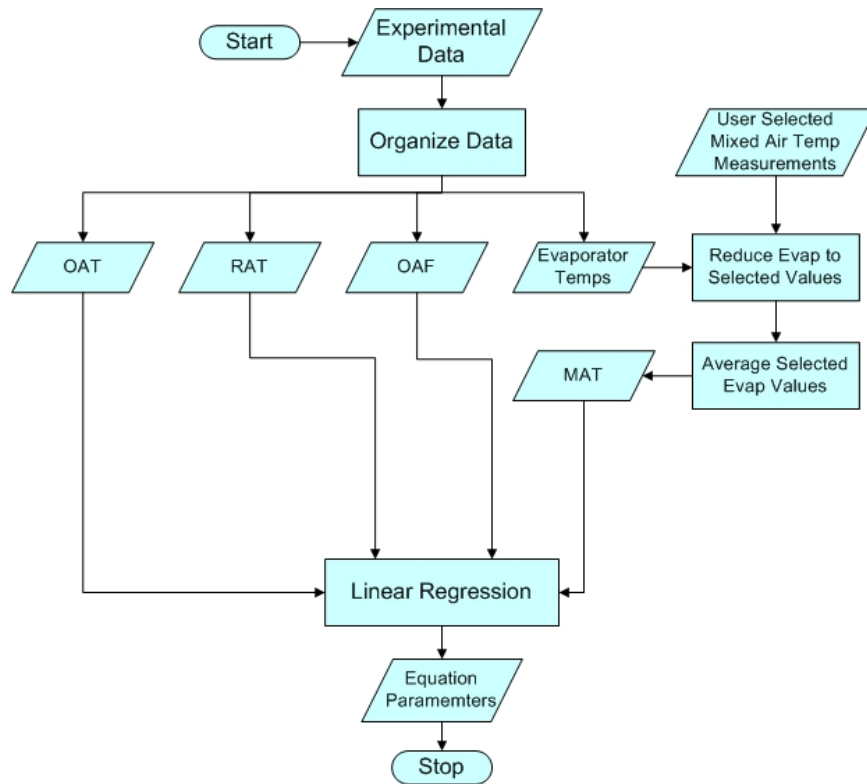


Figure 17: Flowchart illustrating the generation of the economizer equation parameters from experimental data.

When all 15 sensors are selected to generate a MAT, the data fits the equation with an R-squared value of 0.998 and a root mean squared (RMS) error of 0.74°F. Figure 18 shows comparisons of predicted and measured MAT for this case. These results represent the best case for mapping MAT data. The worst case mapping results occur for a single sensor used to characterize MAT. For a single mixed air sensor located at the centerline of the duct (sensor 8), the R-squared value was 0.984 and the RMS-error was 1.95°F. Figure 19 shows comparisons between predicted and measured MAT for this case. These two examples bracket the overall accuracy of the mapping equation.

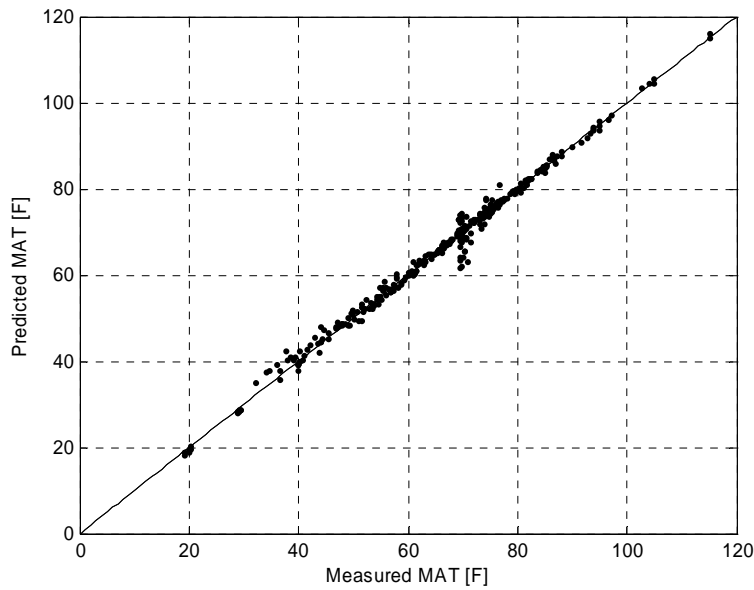


Figure 18: Predicted MAT as a function of measured MAT for all 15 temperature sensors.

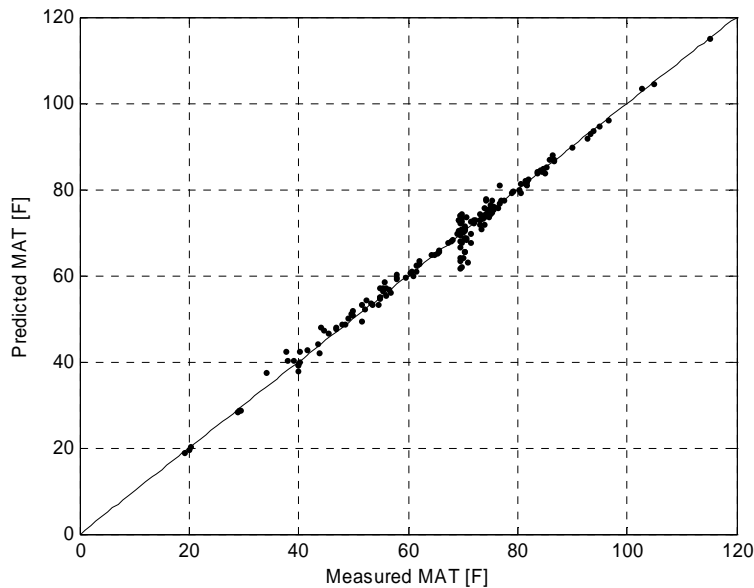


Figure 19: Predicted MAT as a function of measured MAT for temperature sensor number 8.

In this study, both differential dry-bulb and dry-bulb changeover control were considered. Figures 20 and 21 depict the models for each of these cases. Both controllers require specification of a minimum OAF and a setpoint for MAT and use outdoor and return air temperatures as inputs to adjust the OAF according to embedded control logic. The dry-bulb changeover control requires an outdoor changeover setpoint. The outdoor air changeover setpoint specifies the temperature at which the economizer enters

“economizer mode.” Differential dry-bulb control examines the difference between the OAT and RAT and economizer mode is enabled when the difference drops below a setpoint. In economizer mode, the damper is controlled to maintain MAT at the mixed air setpoint. The economizer controller models assume a perfect controller and use the economizer model to determine the OAF necessary to maintain the measured MAT at the setpoint.

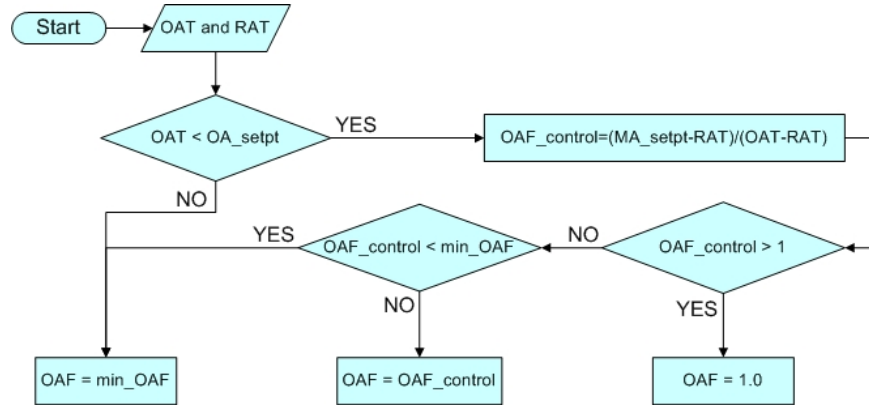


Figure 20: Dry-bulb changeover control modeling logic.

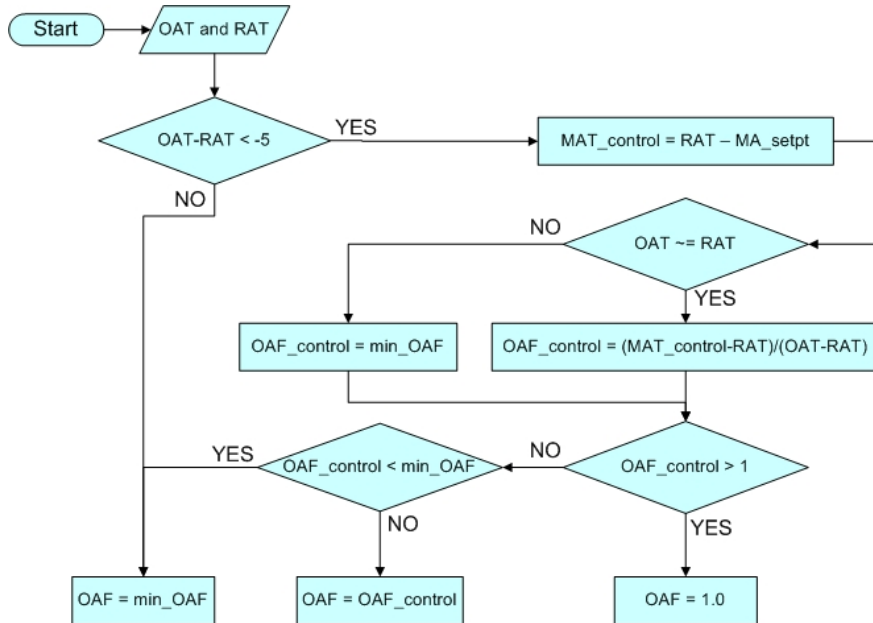


Figure 21: Differential dry-bulb control modeling logic.

The fault implementer allows for single or multiple economizer faults. The most common faults are probably associated with the damper as outlined by Friedman and Piette (2001). Additional faults associated with sensors and the controller were also considered in this study. Eight individual faults were evaluated and categorized as follows:

Sensor Faults

1. Temperature sensor bias
2. Bad sensor
3. Misplaced sensor

Controller Faults

4. Incorrect MAT setpoint
5. Incorrect minimum OAF setpoint

Damper Motor/Actuator Faults

6. Damper motor failure where the damper closes (OAF = 0)
7. Lack of control signal to a powered damper (OAF = minOAF)
8. A physically stuck damper (OAF = constant)

Each of these faults was straightforward to simulate. The sensor bias represents a miscalibrated or improperly working sensor and was implemented as a specified fixed error. The misplaced sensor refers to a sensor that is wired to the wrong channel and was simulated by considering different combinations where the two channels are reading the same value (e.g., the OAT channel reading the RAT). The bad sensor fault represents a total sensor failure and was simulated by setting the sensor output to an artificially high number, 3e20. The incorrect setpoints (faults 4, and 5) were simulated by specifying a fixed bias and represent faults where the economizer system controller setpoints and the setpoints supplied to the FDD algorithm are not the same. These controller faults also could represent problems more physical in nature such as a damper motor potentiometer specifying the minOAF is not set properly. The damper/actuator faults (faults 6, 7, and 8) were implemented by specifying an appropriate fixed damper position.

A summary of the faults and the implementation options are given in Table 5. Combinations of different faults were not considered. However, different fault levels were considered for the sensor bias and incorrect setpoint faults. Fault levels for the sensor bias and incorrect MAT setpoint faults were varied in 5°F increments above and below the nominal level up to 20°. The incorrect minimum OAF setpoint fault level was varied in increments of 5% going below the nominal level 15% and above by 20%. The sensor bias and bad sensor faults also required selection of a sensor to be biased or assumed bad. The OAT, RAT, and MAT sensors could be selected. The misplaced sensor fault used six combinations of misplaced sensors including replacing the OAT with the RAT and MAT, the RAT with the OAT and MAT, and the MAT with the OAT and RAT. The bad sensor fault assumed that the value that the sensor returned was 3e20.

Table 5: Summary of Fault Implementation Options and Fault Levels

Fault	Fault Implementation Options	Fault Levels
Sensor Bias	Sensor Selection, Fault Level	-20 to 20°F
Bad Sensor	Sensor Selection	n/a
Misplaced Sensor	Sensor Misplacement Combination	6 combinations
Incorrect MAT Setpoint	Fault Level	-20 to 20°F
Incorrect minimum OAF Setpoint	Fault Level	-15% to +20%

Damper Motor Failure (OAF=0)	None	n/a
Lack of Control Signal to Damper (OAF=minOAF)	None	n/a
Physically Stuck Damper (OAF=1.0)	None	n/a

Figure 22 gives a flowchart for the overall model. The inputs to the model are the setpoints, number and location of mixed air sensors, the outdoor and return air temperatures, and the faults. The mixed air sensor specification determines the choice of economizer model used to estimate the average mixed air temperature. The controller model uses the setpoints and sensor inputs to determine the appropriate OAF. Sensor faults cause biases to be applied to the OAT, RAT, or MAT values which cause the MAT to deviate from the setpoint. Economizer (motor/actuator) faults result in OAF values that override the controller output.

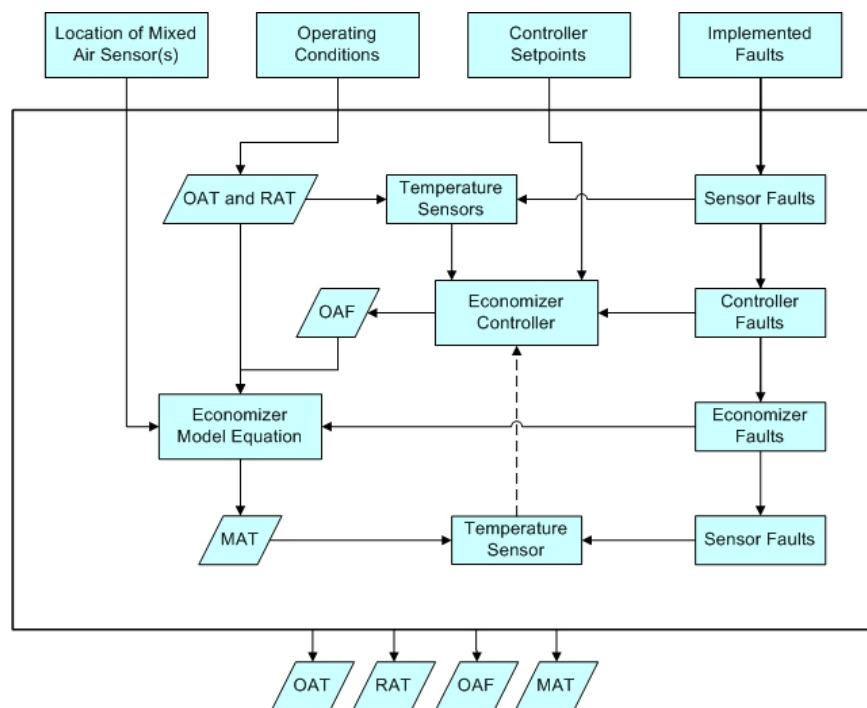


Figure 22: The economizer model with its respective inputs and outputs.

FDD Algorithm Evaluation Process

Figure 23 shows the process used to evaluate the economizer FDD algorithm. The operating conditions, faults to be simulated, and number and location of mixed air sensors are specified as inputs. This information is used within the economizer system model to predict sensor outputs for OAT, RAT, and MAT and the outdoor air fraction which are all inputs to the FDD algorithm. The FDD algorithm acts on this information to predict the occurrence of a fault. All of this information can be input in the economizer model to generate a data set to be input into the FDD algorithm. The algorithm then outputs what it thinks are faulted conditions and presents a diagnosis for the fault. Since the implemented fault was provided, the actual faulted conditions and diagnoses are known. The known faults conditions and algorithm outputs are compared

to determine the effectiveness of the method. The economizer FDD algorithm was evaluated for all eight faults presented in Table 5 for both dry-bulb changeover and differential dry bulb control. The effectiveness of the algorithm was tracked using two parameters: the missed fault rate and the false alarm/false diagnosis rate. The missed fault rate (MF) and the false alarm/false diagnosis rate (FA) in percent were calculated as

$$MF = \frac{N_{\text{missedfaults}} \times 100}{N_{\text{total}}}$$

$$FA = \frac{N_{\text{falsealarm}} \times 100}{N_{\text{total}}}$$

where the number of missed faults is $N_{\text{missedfaults}}$, the number of false alarms/false diagnoses is $N_{\text{falsealarm}}$, and the total number of operating conditions tested for a particular fault is N_{total} .

For each fault examined and at each fault level, at least four different combinations of mixed air sensors were used from the combinations that are listed in Table 6.

Combination	Sensors
1	All
2	3 7 9 13
3	2 4 12 14
4	8
5	3 6 10 13

For all evaluations, the RAT was held constant at 72.5°F (22.5°C) and the OAT was varied from -9°F to 120°F (-22.8°C to 48.9°C). This yields an N_{total} of 130 for each fault test. The minimum outdoor air fraction was set to 0.2 and the dry-bulb changeover setpoint (OAs_{setpt}) for outdoor air was 65°F (18.3°C). The mixed air setpoint (MAS_{setpt}) was set at 55°F (12.8°C) for changeover control, and for differential control, it was set to keep the MAT 20°F below the RAT.

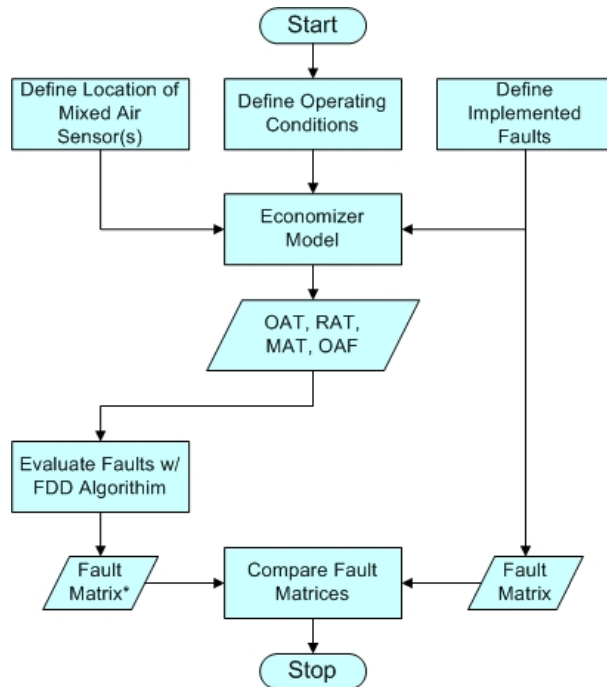


Figure 23: FDD algorithm evaluation process flowchart.

FDD ALGORITHM AND EVALUATION RESULTS

This section presents a description of the original FDD algorithm and evaluation results. In addition, suggested algorithm improvements are described along with their impacts on overall diagnostic performance.

Algorithm Description

The algorithm provided by FDSI is designed to detect problems with an economizer and an air handling unit control system. The algorithm monitors OAT, RAT, and MAT and then estimates OAF from a mass/energy balance. This information is used for economizer diagnostics. In addition, the system monitors the air handling unit's supply air temperature (SAT), thermostat call for cooling or heating, demand control ventilation, and indoor airflow status. Also, the algorithm has built in occurrence criteria so that a fault must be present for a certain period of time for it to be detected. All of these features are important but it is not possible with the experimental data collected to simulate all of the faults outlined in the provided algorithm. The experimental data could only be used for detecting a portion of potential faults related to the economizer only. Also, it is assumed that the economizer system simulated by the model is in steady state and therefore, all of the occurrence criteria in the algorithm were not observed.

The algorithm provided was reduced to the fault detection logic that could be evaluated using the economizer model. The portions of the logic that had time-based elements associated with them were removed. For example, the OAF involved an error calculation which compounded temperature measurement error over time. This error calculation was

removed and approximated by assuming an error of 0.02 F for the OAF. This error is abbreviated as DOAF. Seven of the algorithm’s faults were used and are listed below in Table 7.

Table 7: Fault Criteria of the Provided Algorithm (All temperatures in °F).	
Fault	Fault Criteria
OAT out of range	$OAT < -15$ or $OAT > 125$
RAT out of range	$RAT < (65-1)$ or $RAT > (85+1)$
MAT out of range	if $MAT - RAT \geq -2$ and $MAT - RAT \leq 1$ if $MAT < (OAT - 2.5)$ and $MAT < (RAT - 2.5)$ or $MAT > (OAT + 2.5)$ and $MAT > (RAT + 2.5)$ else if if $MAT < (OAT - 5)$ and $MAT < (RAT - 5)$ or $MAT > (OAT + 5)$ and $MAT > (RAT + 5)$
No Economizer Cooling at Low OAT	$OAT - RAT < -5$ & $OAT > 45$ & $MAT - RAT > -5$
High OAF When High OAT	$OAT - RAT > 5$ & OAF is valid & $OAF - DOAF > 2 * \text{min_OAF}$
Low OAF During Occupied Period	$OAF + DOAF < \text{min_OAF}$
Low Mixed Air Temperature	$MAT < 40$

The OAF is determined using the following logic.

```

if OAT-RAT>=10
    OAF=(MAT-RAT)/(OAT-RAT)
    if OAF<0 and OAF>='Invalid OAF'
        OAF='Invalid OAF'
elseif OAT-RAT<=-5
    OAF=(MAT-RAT)/(OAT-RAT)
    if OAF<0 and OAF>=-1
        OAF='Invalid OAF'
else
    OAF=(MAT-RAT)/(OAT-RAT)
    if OAF<0
        OAF='Invalid OAF'
    else
        OAF='Undetermined OAF'

```

The determination of OAF is performed after the criteria for “no economizer cooling at low OAT” because it is not required until after the first four fault criteria are checked. The OAF calculation will output an invalid or undetermined OAF if the temperature data given is not valid.

Evaluation Results for the FDSI Algorithm

Results for the FDSI algorithm are divided into the three fault groups that were implemented. More detailed results are presented for the damper fault group because the most significant algorithm improvements were identified for this group. All results presented here are for dry-bulb changeover control. An identical evaluation was performed using differential control and the results were very similar.

Damper Fault Evaluation for FDSI Algorithm with Dry-Bulb Changeover Control

The damper system tested in the lab would automatically close if the motor failed so for this fault, the OAF is set to zero and the MAT is calculated to be about the same as the RAT. The missed fault rate for four different mixed air sensor combinations was determined as a function of OAT and is shown in Figure 24 as a function of outdoor air temperature.

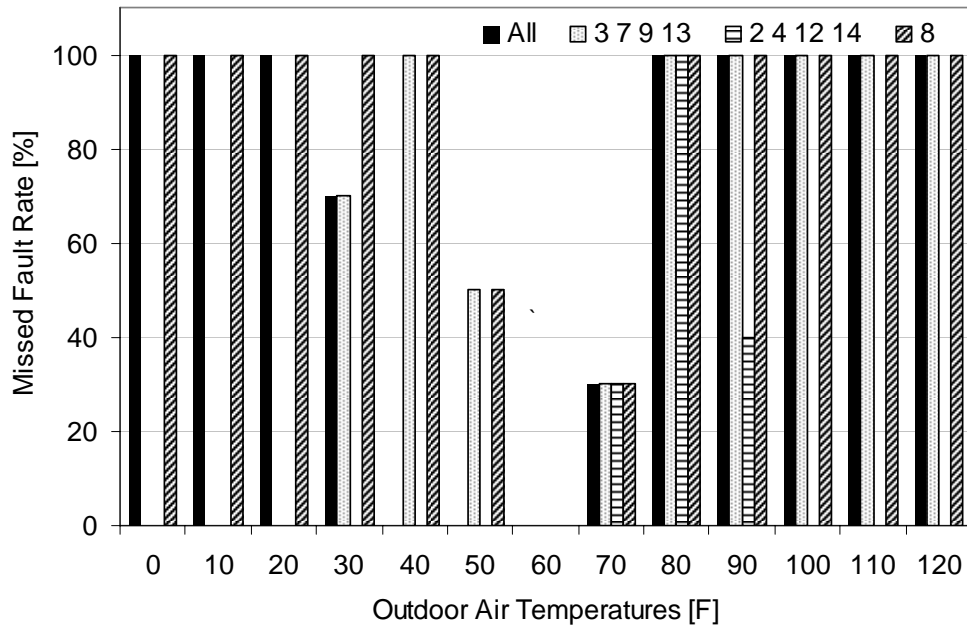


Figure 24: Missed fault rate as a function of OAT for the damper motor failure fault (OAF=0).

This figure shows that for most of the sensor combinations used, the FDD algorithm cannot detect a damper motor failure. The algorithm criteria for this fault is “low OAF during the occupied period,” and the reason that this fault is not detected very well is the fact that the calculation of OAF with the provided temperatures is below zero or higher than one, returning an “invalid OAF.” When the OAF is invalid, the fault cannot be detected.

Without a control signal to the damper motor, the damper will automatically stay at the minimum position. The algorithm had a great deal of trouble detecting this fault because the “no economizer cooling at low OAT” criteria would not detect a fault if the OAT falls below 45°F (7.2°C) and if the MAT is 5° less than the RAT. Also, there is no fault at the higher temperatures because the damper is supposed to be at the minimum position when

the OAT is higher than the RAT. Using sensor 8 only, several false alarms were generated. The results of this fault can be seen below in Figures 25 and 26.

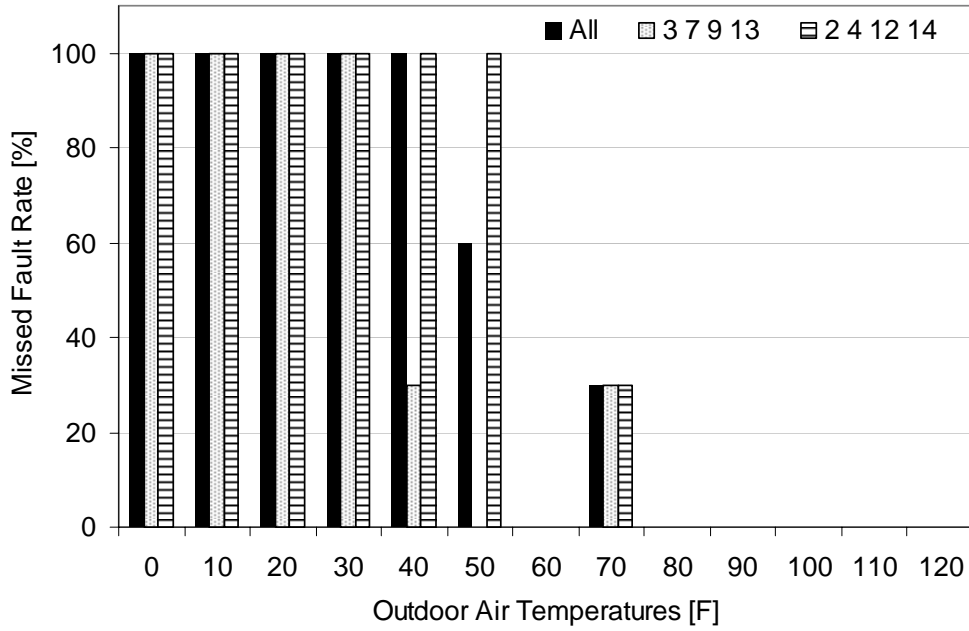


Figure 25: Missed fault rate as a function of OAT for the lack of damper control signal fault (OAF=0.2).

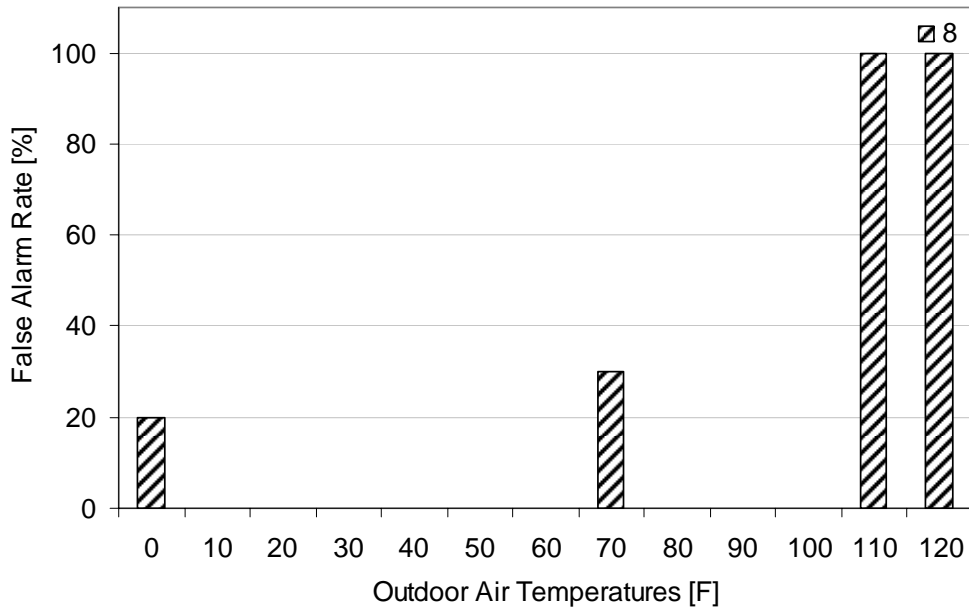


Figure 26: False alarm rate as a function of OAT for the lack of damper control signal fault (OAF=0.2).

A stuck damper was simulated as being stuck in the full open condition. Figure 27 shows results for this fault. The algorithm detected a stuck damper with a little more success than the other two damper faults but still had trouble when the OAT was slightly lower or higher than the RAT. The performance of the algorithm could be improved by adjusting the “low MAT” criterion. The “low MAT” fault setting is 40°F (4.4°C) when it should be set closer to the MAT setpoint. The algorithm cannot detect the stuck damper when the OAT is slightly higher than the RAT due to an undetermined or invalid OAF calculation which cannot be remedied.

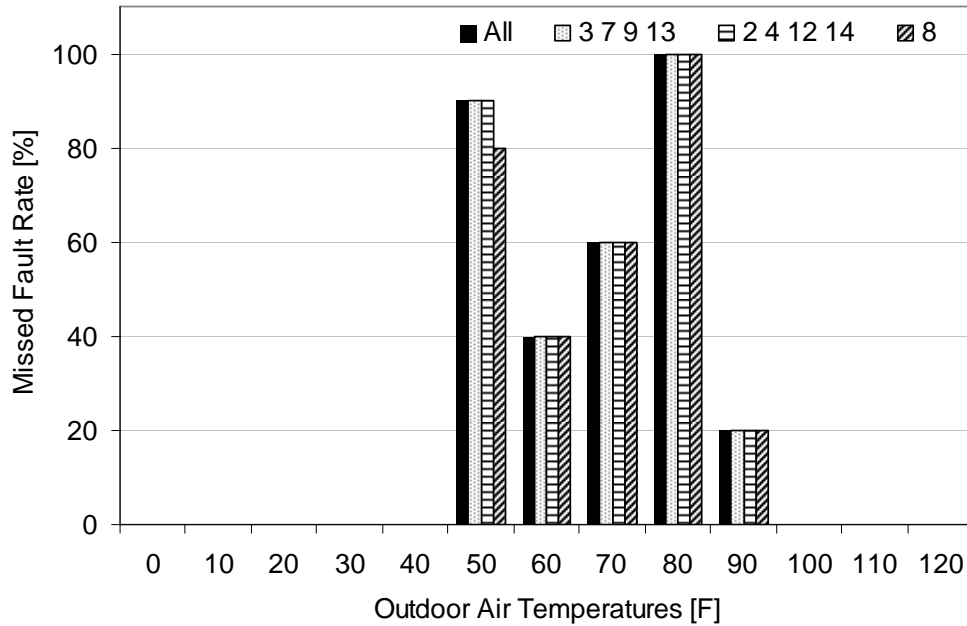


Figure 27: Missed fault rate as a function of OAT for the stuck open damper fault (OAF=1).

Figure 28 presents comparisons of missed fault rates over all values of OAT for each damper fault and sensor combination. The algorithm performed best overall at detecting the stuck open damper and had less success with the other two faults. The other two faults had widely varying results for the different sensor combinations. Since the different sensor combinations take temperature data from different portions of the evaporator grid, the MATs are skewed higher or lower than the real average resulting in a change in performance. This plot also shows that using all of the MAT sensors yields a higher missed fault rate than some of the other sensor combinations which is a result of the mixed air average for the other sensor combinations being skewed so that the algorithm has an easier time detecting the fault. This skewed average also increases the false alarm/false diagnosis rates for those sensor combinations.

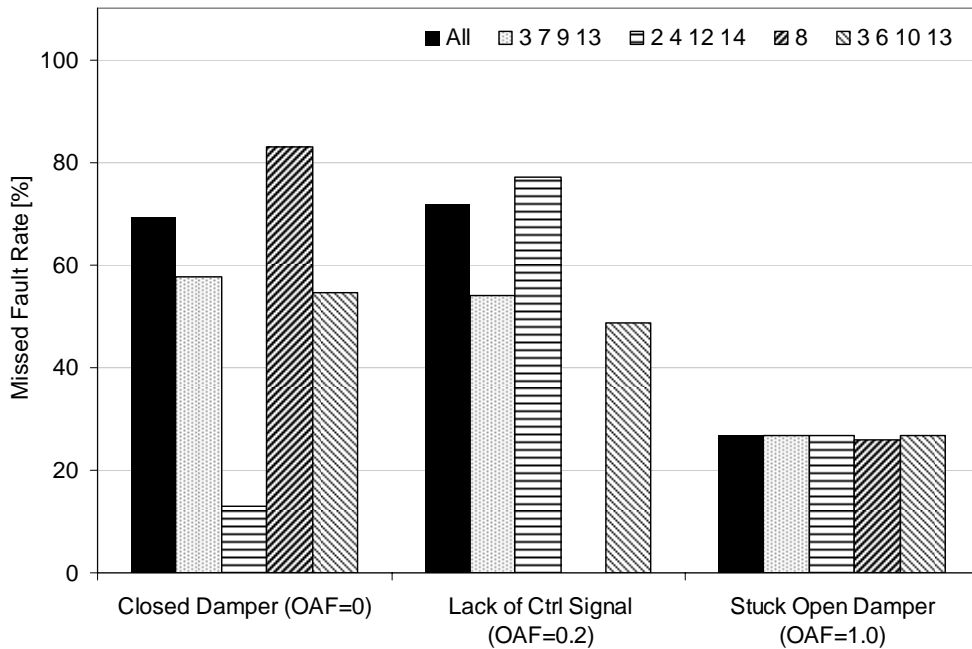


Figure 28: Comparison of missed fault rates for all three faults implemented and different sensor combinations.

Controller Fault Evaluation for FDSI Algorithm with Dry-Bulb Changeover Control

In order to simulate a MAT setpoint fault, the setpoint was raised and lowered from the nominal 55°F (12.8°C) in increments of 5°F (2.8°C) for increasing severity of the fault. Values of the MAT setpoint that are near the normal range would probably not be considered as faults. Also, it would be relatively simple matter to check the validity of a specification for the MAT setpoint. However, for the purposes of highlighting a deficiency of the current algorithm, missed fault detection rate results for this fault are shown in Figure 29. As the setpoint was lowered, the fault was not detected at all until the MAT dropped consistently below the criteria for “low MAT.” On the other hand as the setpoint was raised, there was no way for the original algorithm to detect a fault. .

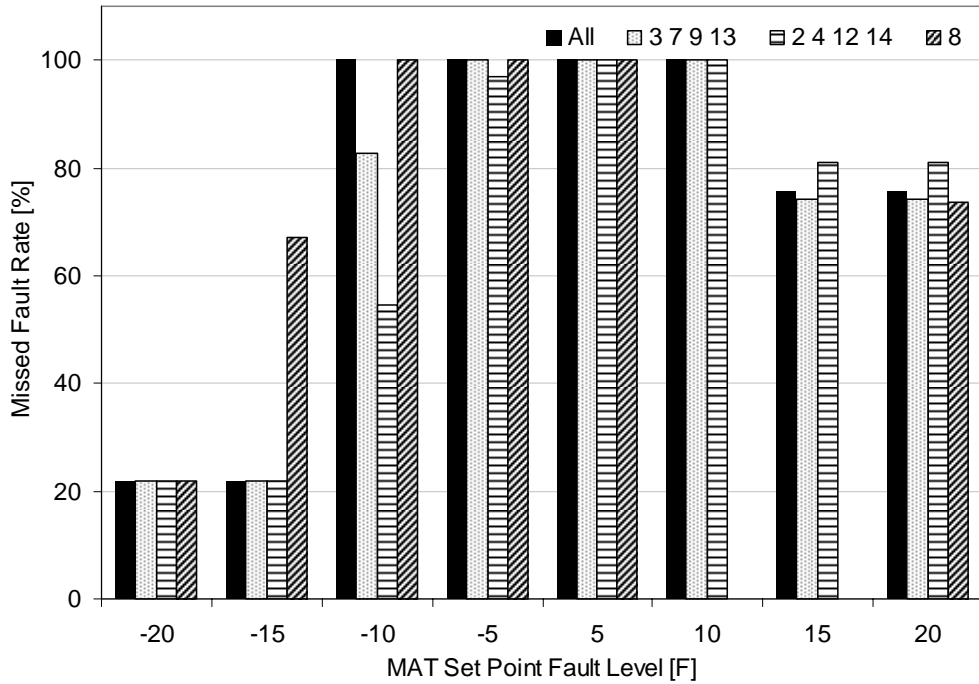


Figure 29: MAT setpoint fault level comparison of missed fault rates for four different MAT sensor combinations.

The minimum OAF fault is similar to the MAT setpoint fault in that the correct setpoint is not known and it is relatively straightforward to check the validity of a minimum damper position setting. However, in order to simulate this fault and highlight deficiencies in the FDD algorithm, the minimum OAF setting was varied from a nominal value of 0.2 in increments of 0.05. Figure 30 gives missed false rate results for the minimum OAF setpoint fault. As the setpoint was increased, the algorithm did not have the capability to detect a high minimum OAF until the “high OAF at high OAT” fault criteria was exceeded. Even then, the algorithm was only able to detect this fault at high OATs. Decreasing the setpoint was easier for the algorithm to detect due to the criteria for the “low OAF during the occupied period.”

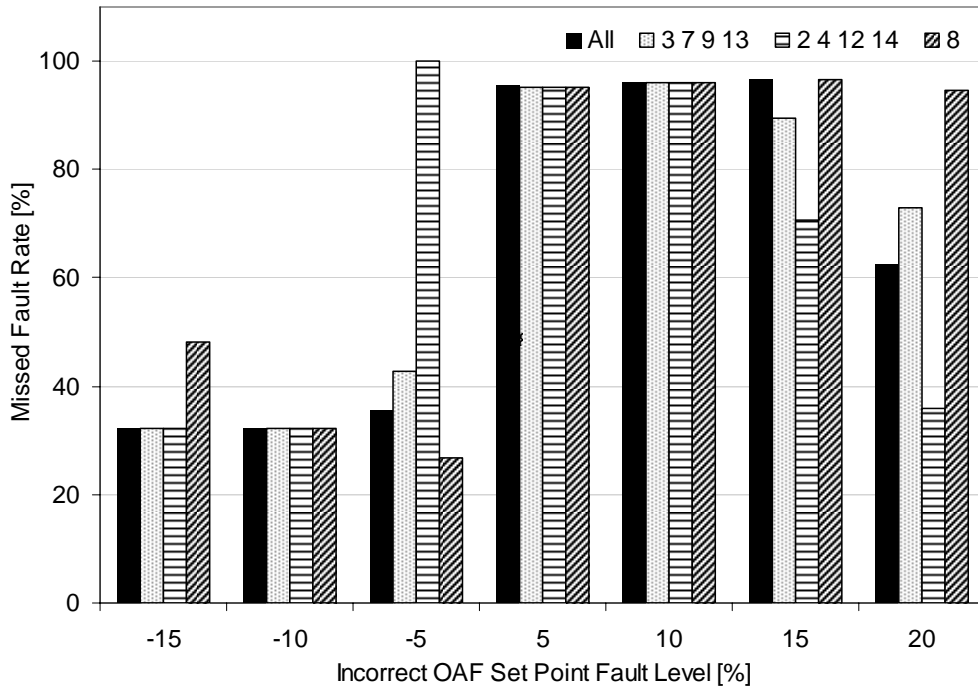


Figure 30: Minimum OAF setpoint fault level comparison of missed fault rates for four different MAT sensor combinations.

Sensor Fault Evaluation for FDSI Algorithm with Dry-Bulb Changeover Control

A bad sensor fault was simulated by replacing the data with an extremely high or low number (e.g., $3e20$ to represent a bad sensor connection to the FDD data acquisition system). The algorithm was able to detect this fault perfectly and so no results are presented.

Misplaced sensor faults were simulated by switching sensor values between channels. Figure 31 shows fault rates for all possible individual sensor switch combinations. This type of fault could only be detected when the RAT sensor was switched with the OAT or MAT sensor, which forced it to be out of its range as specified in the fault criteria. Switching the OAT and MAT sensors did not lead to a fault indication.

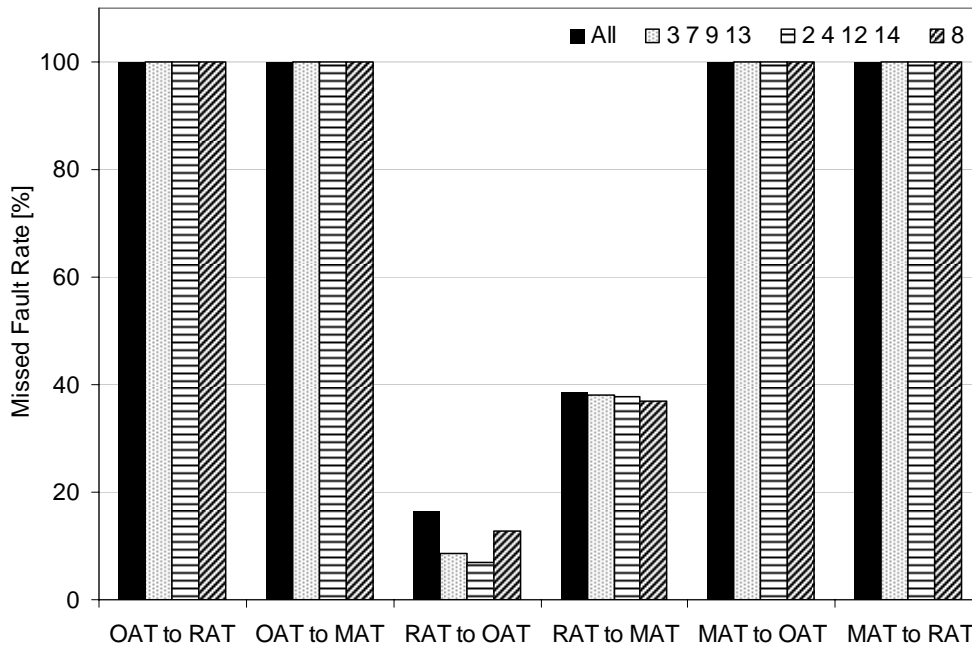


Figure 31: Misplaced sensor fault missed fault rates.

A sensor bias fault was simulated by artificially increasing or decreasing individual temperature sensors. This type of fault could occur in an economizer system when the sensors are not calibrated properly. Figure 32 below shows missed fault rate results as a function of sensor bias applied individual to the OAT, RAT, and MAT measurements. Although all of the 15 MAT sensors were used for these results, similar results were obtained for different MAT sensor combinations. Since the algorithm works off of real time measurements of temperature and has no built in calibration functions, it cannot detect sensor bias faults very effectively. It does a better job of detecting biases in MAT than OAT and RAT. However, the bias needs to be very large before a fault is detected.

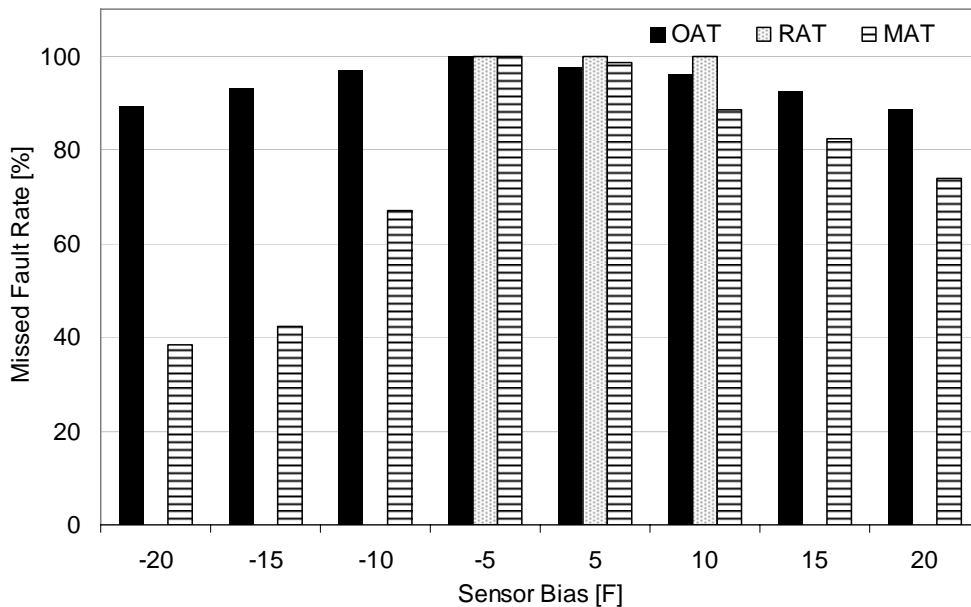


Figure 32: Missed fault rate results for the sensor bias fault using all mixed air sensors.

Suggested FDD Algorithm Improvements

Missed fault rates were high for all of the faults implemented, especially for the damper faults. To improve the algorithm, some of the fault detection logic was rewritten and rearranged. For some, it was enough to just change the fault setpoint to improve detection. Through all of these changes, it was important not to increase the false alarm rate in the process.

Improvements were made to four of the fault criteria and the determination of the OAF. The first fault criterion that was improved was the “low mixed air temperature” fault. It was originally set so that if the MAT fell below 40°F (4.44°C), the fault would register. In unfaulted operation, the MAT should stay close to the MAT setpoint when the damper is being actively controlled. If the MAT falls below the MAT setpoint, it should be considered a fault. The criterion was changed to be within a deadband of 2.5°F (1.39°C) of the MAT setpoint established to prevent false alarms due to measurement error.

Next, the “no economizer cooling at low OAT” fault criterion was improved. This criterion was not designed to use the OAF as it was placed before the determination of OAF in the algorithm. While this makes the criterion for the fault very simple, it limits the ability of the algorithm to detect this fault. One of the original criteria for this fault was that the OAT had to be greater than 45°F (7.22°C). This prevents the algorithm from detecting this fault when outside air is very cold. However, at temperatures lower than 45°F, economizer cooling could still be used to control the MAT to its setpoint. A better lower limit on the OAT for economizer operation can be estimated using an estimate of the minimum OAF, the MAT setpoint, and RAT using

$$OAT > \frac{(MA_{setpt} + (minOAF - 1)RAT)}{minOAF}$$

The fault criteria for a “no economizer cooling at low OAT” also required the OAT to be 5°F (2.78°C) less than the RAT. This criterion was designed for differential control which does not work for changeover control. Adding another criterion for changeover control requiring the OAT to be less than the OAsptpt corrects this problem. Also, moving this fault criterion to a position after the determination of the OAF, the OAF can be used to help determine if there is a fault. This would be done by checking the OAF to see if it is below the minOAF plus 2% which would indicate that the damper is at the minimum position when it should not be.

The algorithm had difficulty in detecting a closed damper fault because the calculated OAF would often be invalid preventing it from being used in detecting faults. The “low OAF during occupied period” fault relies solely on the OAF calculation. The economizer model showed that when the damper was closed, the MAT was often measured to be outside of the range of the OAT and RAT. By adding extra criteria to this fault for the cases where the MAT is not measured to be in between the OAT and RAT, this fault can be detected much more readily.

The last fault criterion to be improved is the “high OAF at high OAT” fault, which did not have a criterion sensitive enough to detect the OAF setpoint fault. The criterion required the OAF to be twice the minimum OAF when the OAT is 5°F (2.78°C) higher than the RAT to be detected. To make it more sensitive, the OAF only has to be 1.25 times higher than the minimum OAF to be detected.

In addition to the improved fault criteria, the OAF determination was rewritten to account for the two different control methods used. It was also simplified. Table 8 shows a summary of all of the improvements made to the fault criteria and the determination of OAF.

Table 8: Fault criteria comparison (All temperatures in °F)

Fault or Calculation	Original	Improved
Low Mixed Air Temperature	MAT<40	ctrl_method='DB changeover' & (MAT+2.5)<MAT_setpt or ctrl_method='Differential DB' & (MAT+2.5)<(RAT-MAT_setpt)
No Economizer Cooling at Low MAT	OAT-RAT<-5 & OAT>45 & MAT-RAT>-5	ctrl_method='DB Changeover' & OAT<OAT_setpt & OAT>(MAT_setpt+(min_OAF-1)*RAT)/min_OAF & OAF<min_OAF+0.02 or ctrl_method='Differential DB' & OAT-RAT<-5 & OAT>(MAT_setpt+(min_OAF-1)*RAT)/min_OAF & OAF<min_OAF+0.02
Low OAF During Occupied Period	OAF+DOAF<min_OAF	OAF+DOAF<min_OAF or OAT-RAT>5 & MAT-0.5<RAT or OAT-RAT<-5 & MAT+0.5>RAT
High OAF When High OAT	OAT-RAT>5 & OAF is valid & OAF-DOAF>2*min_OAF	OAT-RAT>5 & OAF is valid & OAF-DOAF>1.25*min_OAF
Determination of OAF	<pre> if OAT-RAT>=10 OAF=(MAT-RAT)/(OAT-RAT) if OAF<0 and OAF>=-1 OAF=-1 elseif OAT-RAT<=-5 OAF=(MAT-RAT)/(OAT-RAT) if OAF<0 and OAF>=-1 OAF=-1 else OAF=(MAT-RAT)/(OAT-RAT) if OAF<0 OAF='Invalid OAF' else OAF='Undetermined OAF'</pre>	<pre> if (ctrl_method='DB Changeover' & OAT-RAT>=(OAT_setpt-RAT) & OAT-RAT<=10 or ctrl_method='Differential DB' & OAT-RAT>=-5 & OAT-RAT<=10) OAF=(MAT-RAT)/(OAT-RAT) if OAF<0 OAF='invalid OAF' else OAF='undertermined OAF' else OAF=(MAT-RAT)/(OAT-RAT) if oaf(ii)<0 &oaf(ii)>=-1 OAF='invalid OAF'</pre>

Evaluation of the Improved Algorithm

Results for the improved algorithm are organized by fault type and directly compared with previous results to show the improved FDD performance.

Damper Fault Evaluation for Improved Algorithm with Dry-Bulb Changeover Control

The improvements to the algorithm were designed primarily to better detect damper faults and the improvement is dramatic as shown in Figures 33 and 34. Figure 33 shows the impact of sensor choice on the missed fault rate and is directly comparable to Figure 28. Figure 34 shows direct comparisons of results for the FDD algorithms when considering all five sensor combinations.

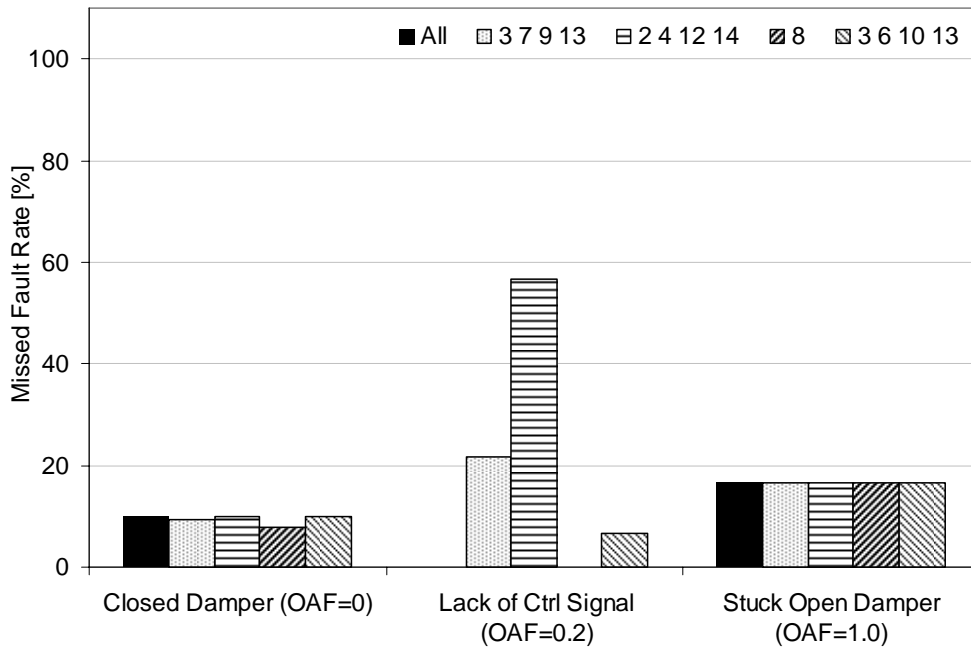


Figure 33: Comparison of missed fault rates for all three faults implemented and different sensor combinations using the improved algorithm.

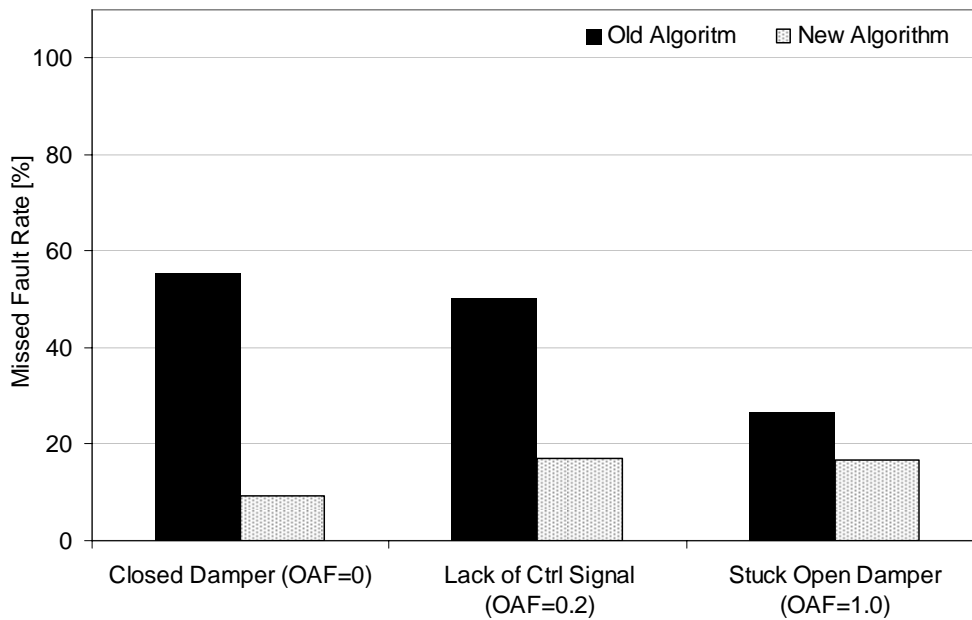


Figure 34: Comparison of the old and new algorithms for each damper fault.

Controller Fault Evaluation for Improved Algorithm with Dry-Bulb Changeover Control

The improved FDD criteria also had a large impact on performance for the controller faults. Improving the “low mixed air temperature” and the “high OAF at high OAT” fault criteria allowed the algorithm to detect and correctly diagnose the controller faults with a greater efficiency. Figures 35 and 36 show comparisons between the old and new algorithms’ missed fault rates for the MAT and minimum OAF setpoint respectively. Selected mixed air sensor combinations are shown because the results were fairly similar to one another.

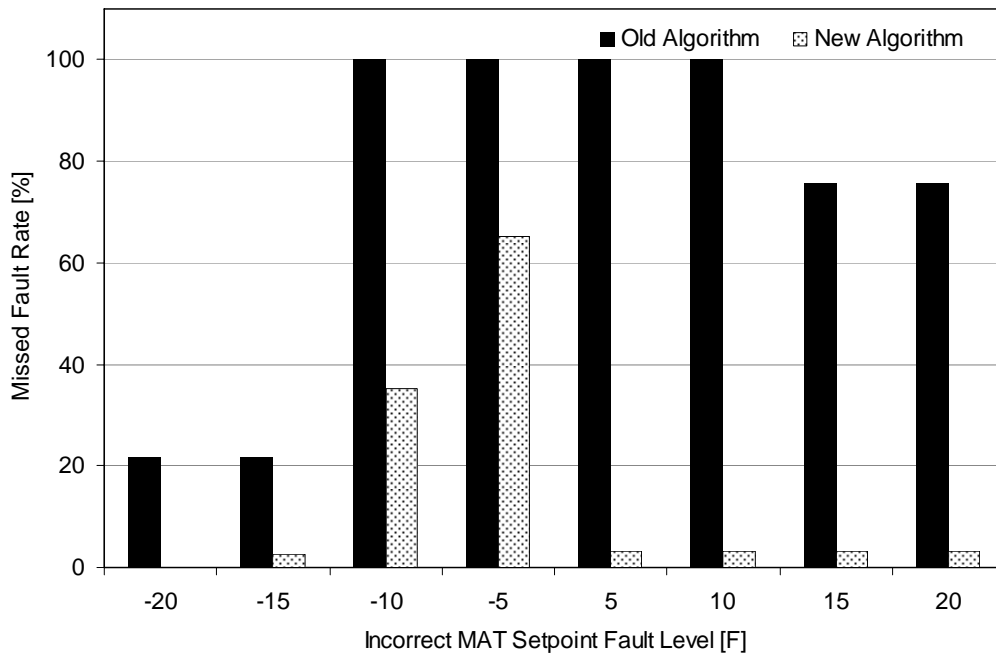


Figure 35: Comparison of old and new algorithm's incorrect MAT setpoint missed fault rate for the sensor combination using all mixed air sensors.

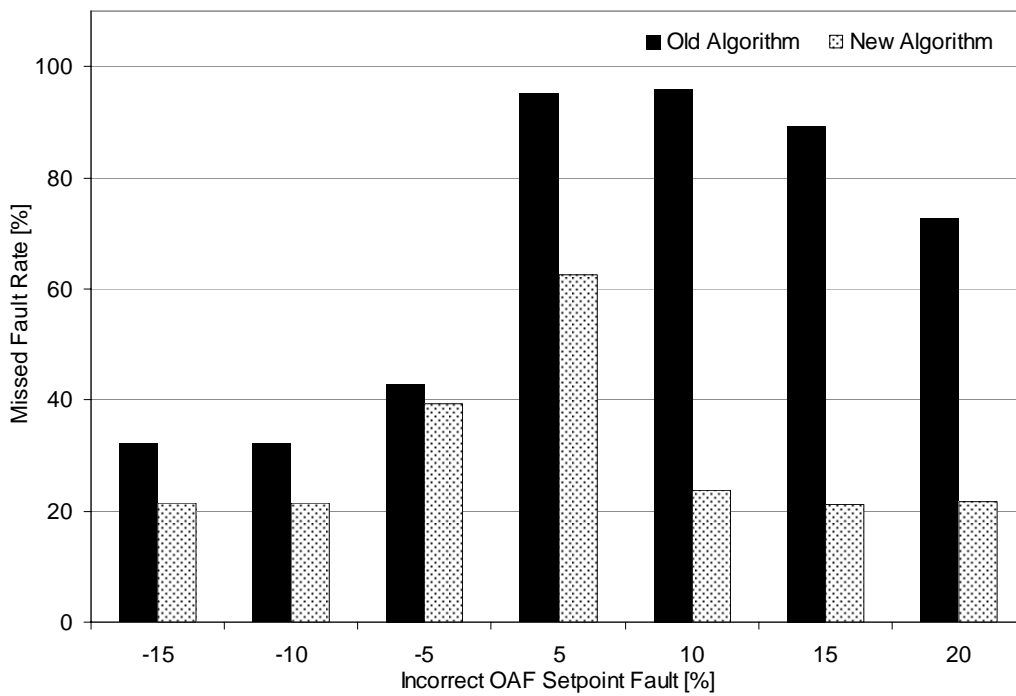


Figure 36: Comparison of old and new algorithm's incorrect OAF setpoint missed fault rate for the sensor combination using mixed air sensors 3, 6, 10, and 13.

Sensor Fault Evaluation for Improved Algorithm with Dry-Bulb Changeover Control
Improvements to the FDD algorithm had little effect on performance for detecting sensor faults. The current algorithm sets specific ranges of acceptable temperature measurements and adjusting these to better detect a fault like sensor bias is not practical. Figures 37 and 38 show comparisons between performance for the original and improved algorithms with sensor faults. In this case, there is little very improvement in performance for the improved algorithm.

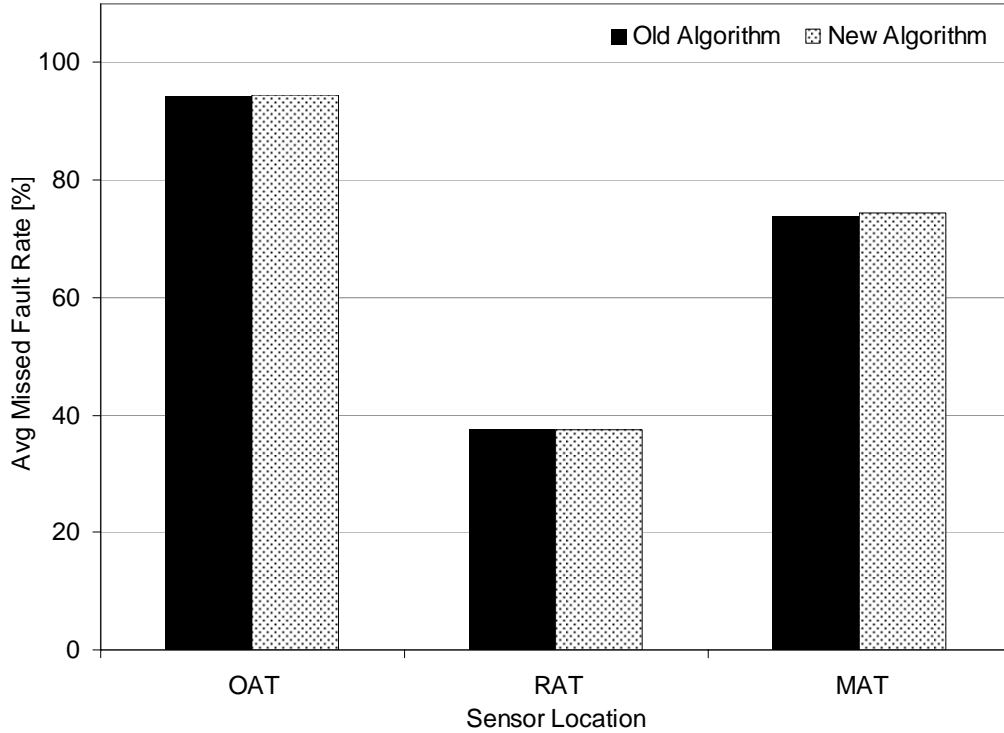


Figure 37: Comparison of missed fault rates averaged over all sensor combinations and fault levels of the sensor bias fault.

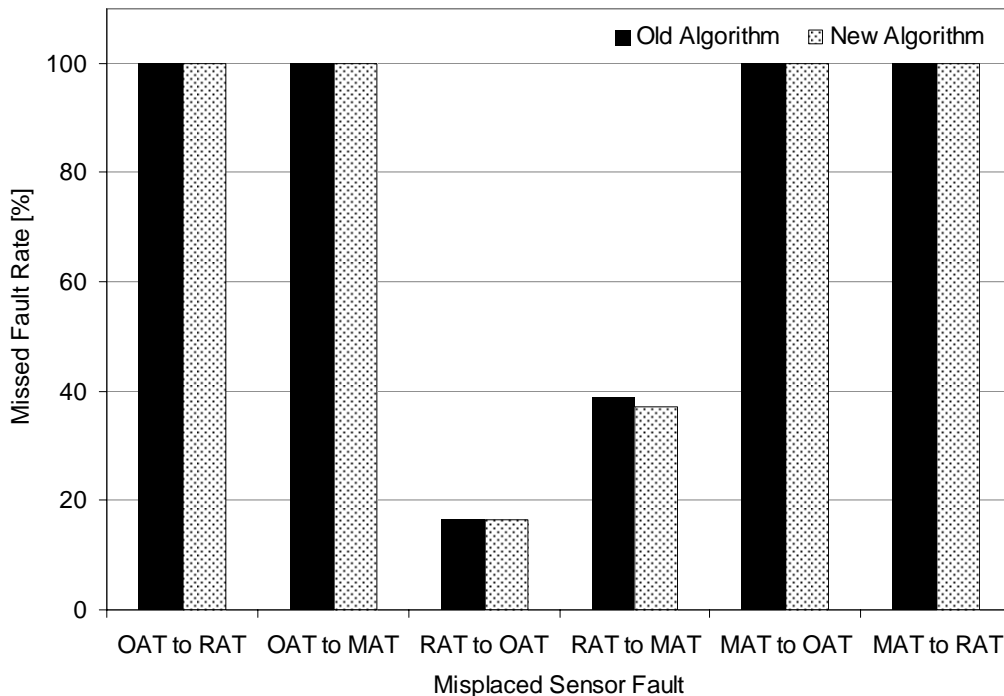


Figure 38: Comparison of missed fault rates averaged over all sensor combinations of the misplaced sensor fault.

Summary of Results

Figure 39 shows a summary comparison of missed fault rates for the two algorithms for dry-bulb changeover control. When the results are averaged over all sensor combinations, fault levels, and faults implemented the missed fault rate is reduced from 59.25% to 33.12%. If just the damper and controller faults are considered, the average missed fault rate improves from 54.37% to 18.73%. This larger improvement is expected since the algorithm was changed to specifically improve detection of these two types of faults. It would be difficult to improve the missed fault rate much more than this because no matter what fault is implemented, there is always a range of OATs where the OAF cannot be accurately determined. This range makes up about 13% of all of the supplied operating conditions and sets a limit on how much the algorithm can be improved.

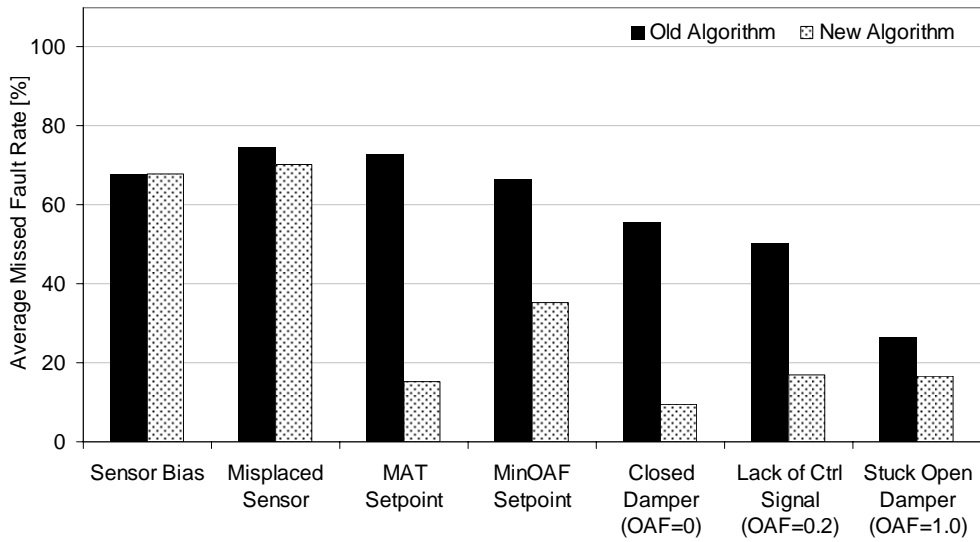


Figure 39: Comparison of the missed fault rates for every fault implemented averaged over all fault levels and sensor combinations using dry-bulb changeover control.

One of the concerns with changing the FDD algorithm was that even though missed fault rates would decrease, it could make the algorithm more susceptible to false alarms and false diagnoses. Figure 40 shows false alarm rate comparisons for the two methods for all faults considered. The new algorithm did slightly increase the overall false alarm/false diagnosis rates using dry-bulb changeover control from 9.10% to 10.60%. Most of the increase occurred in the sensor faults. The damper and controller faults were not greatly affected.

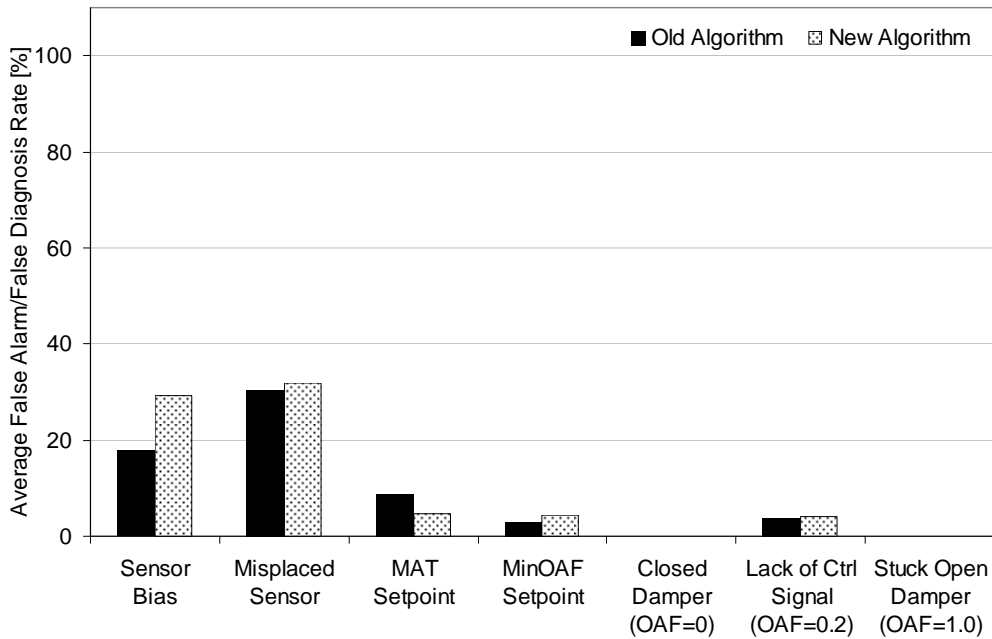


Figure 40: Comparison of the false alarm/false diagnosis rates for every fault implemented averaged over all fault levels and sensor combinations using dry-bulb changeover control.

Differential dry-bulb control yielded similar missed fault and false alarm rate results to dry-bulb changeover control. The amount of missed fault rate improvement between FDD algorithm versions was also comparable between control schemes. The overall average missed fault rate improved from 63.39% to 33.45%. Considering just the damper and controller faults, the missed fault rate went from 60.01% for the original algorithm to 18.04% with the improved algorithm. Using differential control, the false alarm/false diagnosis rates improved slightly between algorithms from 10.64% to 10.39%. It is more important to note that the algorithm changes did not have a significant effect on the false alarm rate. Figures 41 and 42 show the missed fault rate and false alarm/false diagnosis rate comparison for differential dry-bulb control.

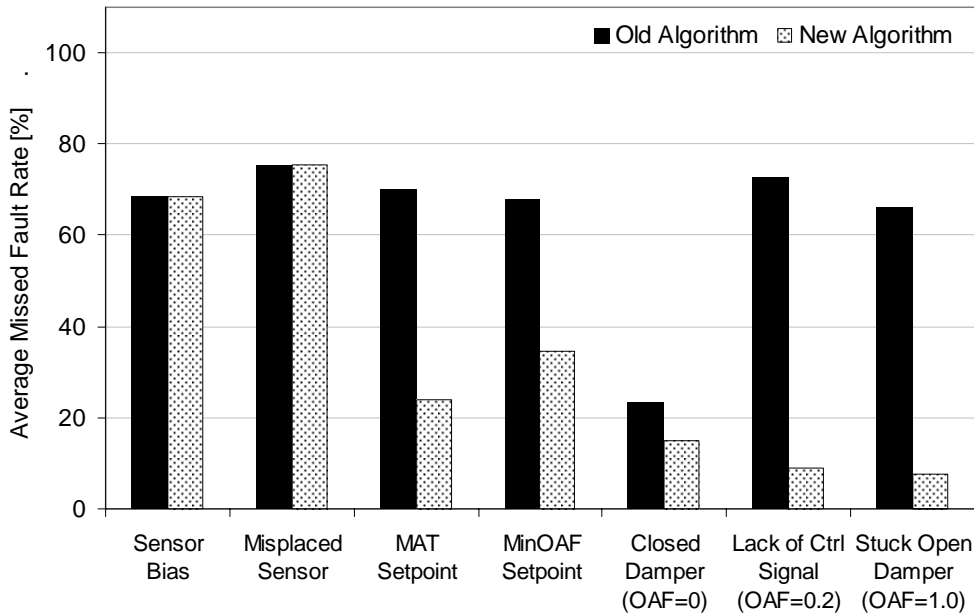


Figure 41: Comparison of the missed fault rates for every fault implemented averaged over all fault levels and sensor combinations using differential dry-bulb control.

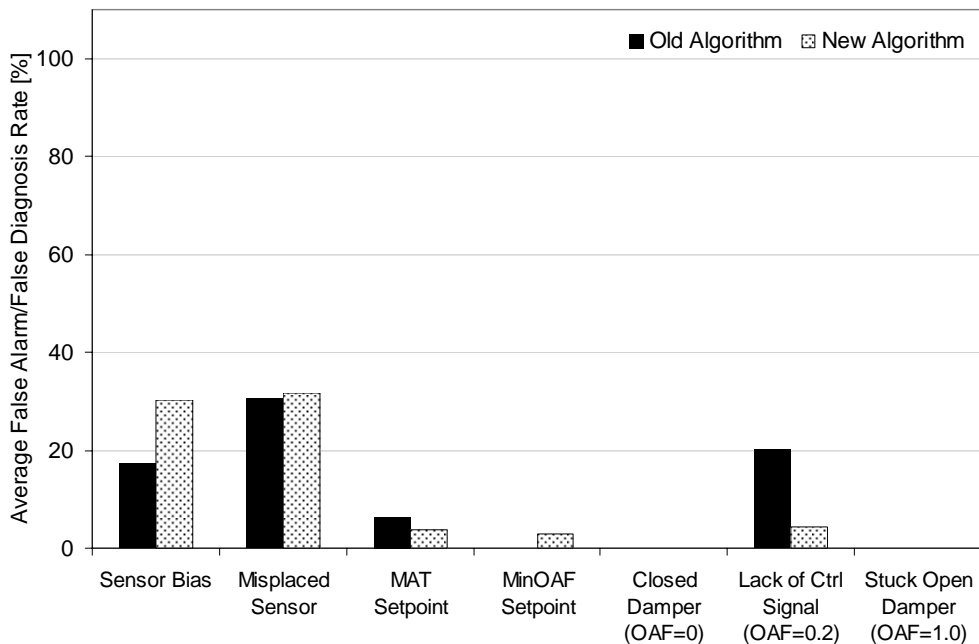


Figure 42: Comparison of the false alarm/false diagnosis rates for every fault implemented averaged over all fault levels and sensor combinations using differential dry-bulb control.

A Description of Other Possible Economizer FDD Methods

According to the evaluation results, the algorithm could use improvement in the area of detecting sensor faults. Through the course of the evaluation, some additional improvements were conceptualized to detect faults with the damper and sensors.

Improving Detection of the Sensor Faults

Two methods are suggested for improving the detection of sensor faults. The first method is designed to improve detection of a misplaced temperature sensor. When a temperature sensor has been physically placed in the wrong location in the system, it is likely that two temperature sensors in the system will be read almost the same value no matter what the operating conditions of the system may be. For example, if the outdoor air sensor was removed during a routine maintenance then replaced in the return air position, both the OAT and RAT would read about the same temperature in the return air duct. This by itself cannot be detected with the current FDD algorithm, but if a new fault criterion were added specifically looking for this over a long period of time, it would be possible to detect this problem. The new criterion could look for two of the economizer system temperatures to stay within 2°F (1.11°C) for a 24 hour period. Over the course of a typical day, the OAT and MAT should have more than a 2°F temperature change. Therefore, the misplaced sensor fault could be detected.

To detect bias in the sensors would require a different approach than just adding a new fault criterion. Adding a sensor calibration procedure into the FDD algorithm would allow detection of sensor problems. To calibrate the sensors, the algorithm would require an internet connection to determine local weather conditions and active damper control.

First, the local OAT would be obtained from an internet source. Then, the damper would be placed in the fully open condition, making the OAF equal to 1.0 and the OAT equal to the MAT. The weather station can then be compared with the measured system OAT and MAT. If they are all equal within some tolerance for error, the damper would then be closed. With an OAF equal to 0.0 and the MAT theoretically equal the RAT and the MAT's accuracy verified, the measured system MAT can be compared to the RAT to check for a fault. If any of the sensors fail this check, all of the sensors should be examined for faults. This sensor calibration procedure could be performed at regular intervals as part of a maintenance routine to insure there is no sensor bias in the economizer system.

An Alternate Method for Detecting Damper Faults

The current economizer algorithm uses simple rules based on the OAT, RAT, MAT, and calculated OAF to detect faults with the damper. It is also possible to determine an "expected" value for OAF (OAF_{spt}) that is based on the MAT setpoint and measurements of OAT and MAT. The current OAF could be compared with OAF_{spt} to identify a fault. For example, if the OAF should be 0.7 but it is calculated to be 0.21, this would clearly indicate no economizer cooling at a low OAT fault. This technique could be integrated into the current algorithm and provide a simple warning message stating that the damper is out of position. Then, the current fault logic could be used to perform the diagnosis.

SUMMARY, CONCLUSIONS, AND RECOMMENDATIONS

Summary and Conclusions

The two goals of this project were to assess the accuracy of different temperature and dew point measurement methods in the mixing chamber of the economizer system and to evaluate an economizer FDD algorithm. The experiments conducted with this research helped accomplish both of these goals. Temperature and dew point data collected in the mixing chamber of the roof top air conditioner were used to evaluate the accuracy of single-point and four-point temperature measurements as well as a two-point dew point measurement. Then, a model of the economizer was created by using all of the data collected in the experiment.

Results of the experiments showed that the temperature sensor combination comprised of sensors located symmetrically around the center of the duct (sensors 3, 6, 10, and 13) provided the closest representation of the full 15-point average. However, other four-point combinations showed similar results. Using the best four-point combination, the average difference between the four-point and 15-point combinations never exceeded 2°F (1.11°C). For the majority of the outdoor air conditions tested, the difference was well under that maximum difference, making it, along with the other four-point combinations, an accurate representation of the mixed air temperature. The dew point results were also promising. A two-point dew point measurement method was selected and compared to the 10-point measurement. These measurements were used to calculate air enthalpies and results showed that the two-point method always stayed within 1.1% of the 10-point method on average. Furthermore, the use of a single moisture measurement located at the

centerline of the duct would give similar results. The two-point method was used throughout the testing after this was performed. After the testing was completed, an energy balance showed that the measured Mh stayed within 1.1 Btu/lb (2.56 kJ/kg) of the calculated Mh.

Using the experimental data, an economizer model was created so that faults could be simulated and the FDD algorithm could be evaluated. The economizer experiments, in addition to the literature, provided useful insights into creating a list of faults to implement within the economizer model. Eight different faults were simulated using five different combinations of mixed air temperature sensors. This was done for both dry-bulb changeover and differential dry-bulb control methods. The provided algorithm was evaluated, and then improved upon by fixing weaknesses in the algorithm's logic, and another evaluation was performed using the improved algorithm. The improved FDD algorithm resulted in a 26% decrease in missed faults when using dry-bulb changeover control, and a 30% decrease when using differential dry-bulb control. False alarm and false diagnosis rates were not significantly changed as a result of the algorithm improvements.

Recommendations

Based on the experiments and algorithm evaluations, the following recommendations are offered:

- Using a single dew-point or humidity sensor at the center of the mixed air measurement grid will give accurate mixed air measurements.
- A single temperature sensor could be used for finding the mixed air temperature, but large errors would be incurred at the high and low extremes of the outdoor air temperature. Using any logical four-point combination of sensor would be a significant improvement in accuracy over just one sensor.
- Improving the economizer FDD algorithm by the ways described in Table 8 allow for lower missed fault rates and no significant change to the false alarm and false diagnosis rates.
- Using suggested techniques to better detect sensor faults should be incorporated into the algorithm.

NOMENCLATURE

%OA	= Percent outdoor air
DOAF	= Assumed error in the outdoor air fraction
FA	= False alarm/false diagnosis rate
FDD	= Fault detection and diagnosis
IAQ	= Indoor air quality
\dot{m}_{OA}	= Mass flow rate of the outdoor air
\dot{m}_{RA}	= Mass flow rate of the return air
\dot{m}_{Total}	= Total system air mass flow rate
MAspt	= Mixed air control setpoint
MAT	= Mixed air temperature
MF	= Missed fault rate
Mh	= Mixed air enthalpy
minOAF	= Minimum outdoor air fraction
$N_{falsealarm}$	= Number of false alarms/false diagnoses detected
$N_{missedfaults}$	= Number of missed faults detected
N_{total}	= Total number of operating conditions tested
OAF	= Outdoor air fraction
OAF_control	= Control variable that is compared to the calculated outdoor air fraction
OAFspt	= Expected OAF value
OAspt	= Outdoor air control setpoint
OAT	= Outdoor air temperature
Oh	= Outdoor air enthalpy
RAT	= Return air temperature
Rh	= Return air enthalpy
RMS	= Root mean squared
SAT	= Supply air temperature

REFERENCES

ASHRAE. 2001. ASHRAE Handbook: Fundamentals. Atlanta: American Society of Heating, Refrigeration, and Air Conditioning Engineers, Inc.

Cowan, Alan. October 8, 2004. Report to the Northwest Power and Conservation Council on the review of commercial roof top unit field studies. New Buildings Institute. White Salmon, Washington.

Fisk, W.J., O. Seppanen, D. Faulkner, J. Huang. 2005. Economic benefits of an economizer system: Energy savings and reduced sick leave. *ASHRAE Transactions* 111(2): 673-679.

Friedman, H., M.A. Piette. 2001. Comparative Guide to Emerging Diagnostic Tools for Large Commercial HVAC Systems. LBNL Report 48629, Lawrence Berkeley National Laboratory. Berkeley, CA. May 2001.

Katipamula, S., R.G. Pratt, D.P. Chasin, Z.T. Taylor, K. Gowri, M.R. Brambley. 1999. Automated Fault Detection and Diagnostics for Outdoor-Air Ventilation Systems and Economizers: Methodology and Results from Field Testing. *ASHRAE Transactions* 105(1): 555-567.